UNIVERSITÀ DEGLI STUDI DI MILANO

SCUOLA di DOTTORATO

IN MEDICINA MOLECOLARE E TRASLAZIONALE

Dipartimento di Fisiopatologia Chirurgica e dei Trapianti

CICLO XXXI
Anno Accademico 2017/2018

TESI DI DOTTORATO DI RICERCA

Settore Scientifico Disciplinare **MED/08**

INSIGHTS INTO THE NON-CODING GENOME OF PARATHYROID TUMORS

Dottorando: **Annamaria MOROTTI**

Matricola N° **R11312**

Tutor: Dott.ssa Valentina VAIRA

Co-Tutor: Prof.ssa Monica MIOZZO

Coordinatore del Corso di Dottorato: Prof. Riccardo GHIDONI

ABSTRACT

Recently, long non-coding RNAs (lncRNAs) have been implicated in the regulation of several physiological processes such as cell growth, differentiation and proliferation. Although lncRNAs functions in human diseases have not been completely disclosed, some lncRNAs have already been identified as prognostic and diagnostic biomarkers in different tumors. LncRNAs have also a crucial role in normal development of endocrine organs and their role in endocrine cancer pathogenesis is emerging.

Parathyroid tumors are rare and heterogeneous diseases characterized by genetic and epigenetic alterations resulting in aberrant expression of both protein coding and non-coding genes. Tumors of the parathyroid glands show a great variability in clinical features such as parathormone (PTH) secretion, in the pattern of cell proliferation and in the genetic background. Mutations in the oncosuppressor CDC73 are key events in most carcinomas whereas alterations in the tumor suppressor Multiple Endocrine Neoplasia 1 (MEN1, located at 11q13.1) occur in up to a third of sporadic adenomas. Although lncRNAs play a regulatory role in endocrine cancer pathogenesis, a lncRNAs profiling in human parathyroid tumors is missing. Therefore, we investigated known lncRNAs expression in a series of normal (PaN) and pathological (adenomatous, PAd, and carcinomatous, PCa) parathyroid glands and correlated their expression with cytogenetic aberration, CDC73 status and MEN1 level. Then, we modulated epigenetic complexes and MEN1 expression to get preliminary insights into HAR1B ncRNA functions in parathyroid pathobiology.

We found that a nine-lncRNAs signature distinguishes normal parathyroid glands from parathyroid tumors and also more aggressive tumors from indolent ones. Specifically, KCNQ1OT1 and SNHG6 are enriched in PaNs, HAR1B, HOXA3as, MEG3 and NEAT1 expression characterize PAds, whereas BC200 and HOXA6as are significantly upregulated in PCas compared to PaNs. When this signature was analyzed in a second set of samples, that included also atypical PAds (aPAds), unsupervised analysis showed 3 main samples clusters in which PaNs, all grouped in cluster 2, are distinctly separated from PCas and aPAds, both in cluster 1 and 3. Notably, samples with lncRNAs overexpression, grouped in cluster 3, are characterized by a lower age of tumor onset. Of note, validation analysis highlights a different lncRNAs expression pattern in PCas according to CDC73 gene mutation status. Specifically, CDC73-mutated carcinomas are grouped in cluster 3 and overexpress the majority of the lncRNAs. Moreover, CDC73-mutated PCas display an increment in PTH, calcium serum and ionized calcium levels.

Conversely, lncRNAs expression in adenomas is highly heterogeneous. Therefore, we further characterized this tumor type by performing array Comparative Genomic Hybridization (aCGH). This analysis revealed that chromosome 11 loss of heterozygosity (Chr11-LOH) is the main chromosomal aberration among PAds (10 out of 24 PAds; 42%). Interestingly, Chr11-LOH is associated to a significative HAR1B upregulation. Based on these observations, we analyzed possible regulators of HAR1B expression and we found that HAR1B promoter is a target of EZH2, the

catalytic subunit of the Polycomb Repressive Complex 2. Selective inhibition of EZH2 with Tazemetostat in HEK293 cells restored HAR1B expression levels. In line with this, PAds with Chr-11 LOH show a downregulation of H3K27me3, the direct target of EZH2 activity, compared to PAds without Chr11-LOH. Moreover, HAR1B levels increase after silencing of MEN1 in primary parathyroid adenoma cultures.

Overall, these data shed light on lncRNAs deregulation in human parathyroid tumors and suggest an important role of HAR1B in parathyroid pathobiology.

SOMMARIO

Recentemente, gli RNA lunghi non codificanti (lncRNAs) sono stati implicati nella regolazione di una serie di processi fisiologici tra cui la crescita, il differenziamento e la proliferazione cellulare. Nonostante le funzioni dei lncRNAs nelle patologie umane non siano ancora state rivelate, alcuni lncRNAs sono stati identificati come biomarcatori prognostici e diagnostici in diversi tumori. I lncRNAs hanno anche un ruolo cruciale nel normale sviluppo degli organi endocrini e il loro ruolo nella patogenesi dei tumori endocrini sta emergendo.

I tumori delle paratiroidi sono patologie rare ed eterogenee caratterizzate da alterazioni genetiche ed epigenetiche risultanti nell'espressione aberrante di geni codificanti e non codificanti proteine. I tumori delle ghiandole paratiroidi mostrano una grande variabilità nelle caratteristiche cliniche come la secrezione del paratormone (PTH), nella proliferazione cellulare e nel contesto genetico. Mutazioni nell' oncosoppressore CDC73 rappresentano eventi chiave nella maggior parte dei carcinomi mentre alterazioni nell'oncosoppressore Neoplasia Endocrina Multipla 1 (MEN1, che mappa sul braccio lungo del cromosoma 11, nel locus 13.3) avvengono in circa un terzo degli adenomi sporadici. Nonostante i lncRNAs abbiano un ruolo regolatorio nella patogenesi dei tumori endocrini, un loro profilo di espressione nei tumori umani delle paratiroidi è mancante. A tale scopo, abbiamo analizzato l'espressione di lncRNAs noti in una serie di ghiandole di paratiroide normale (PaN) e patologica (adenoma, PAd, e carcinoma, PCa) e correlato la loro espressione all' alterazione citogenetica, allo stato del CDC73 e al livello di MEN1. In seguito, abbiamo alterato l'espressione dei complessi epigenetici e di MEN1 per ottenere approfondimenti preliminari sulle funzioni del lncRNA HAR1B nella patobiologia della paratiroide.

Abbiamo evidenziato che il profilo di espressione di 9 lncRNAs distingue le ghiandole paratiroidi normali dai tumori delle paratiroidi e anche i tumori più aggressivi da quelli meno aggressivi. In particolare, KCNQ1OT1 e SNHG6 sono arricchiti nei PaNs, l'espressione di HAR1B, HOXA3as, MEG1 e NEAT1 caratterizza i PAds, mentre BC200 e HOXA6as sono significativamente overespressi nei PCas rispetto ai PaNs. Quando il profilo di espressione è stato validato in una seconda casistica di campioni, che include anche gli adenomi atipici (aPAds), l'analisi non supervisionata ha evidenziato 3 principali gruppi in cui i PaNs, tutti raccolti nel gruppo 2, sono distintamente separati dai PCas e dagli aPAds, entrambi nei gruppi 1 e 3. Degno di nota, l'analisi di validazione evidenzia un differente profilo di espressione dei lncRNAs nei PCas secondo la mutazione nel gene CDC73. In particolare, i carcinomi mutati per il gene CDC73 sono raggruppati nel gruppo 3 e ovresprimono la maggior parte dei lncRNAs. Inoltre, i PCas con mutazioni in CDC73, mostrano un aumento nei livelli di PTH, calcio sierico e ionizzato.

Inoltre, l'espressione dei lncRNAs negli adenomi è altamente eterogenea. Quindi, abbiamo caratterizzato questi tumori attraverso la tecnica dell'Ibridazione Genomica Comparativa (aCGH). Questa analisi ha evidenziato come la perdita di eterozigosi (LOH) del cromosoma 11 sia l'aberrazione cromosomica principale tra gli adenomi

(10 su 24 adenomi; 42%). Interessante, LOH del cromosoma 11 è associata ad un significativo aumento di HAR1B. Basandoci su questa osservazione, abbiamo analizzato alcuni possibili regolatori dell'espressione di HAR1B e abbiamo trovato che il promotore di HAR1B è target di EZH2, la subunità catalitica del complesso repressivo Polycomb 2. L'inibizione selettiva di EZH2 con Tazemetostat nelle cellule HEK293 ristabilisce i livelli di espressione di HAR1B. In linea con questo dato, gli adenomi caratterizzati da LOH del cromosoma 11 mostrano una diminuzione dei livelli di H3K27me3, target diretto dell'attività di EZH2, rispetto agli adenomi senza LOH. Inoltre, i livelli di HAR1B aumentano dopo silenziamento di MEN1 in cellule primarie di adenoma, in coltura.

Complessivamente, questi dati pongono luce sulla deregolazione dei lncRNAs nei tumori umani delle paratiroidi e suggeriscono un importante ruolo di HAR1B nella patobiologia della paratiroide.

INDEX

1. INTRODUCTION 1

1.1 Parathyroid glands 1

1.2 Tumors of parathyroid glands 2

1.2.1 Parathyroid adenomas 3

1.2.2 Parathyroid carcinomas 4

1.3 Epigenetic 5

1.3.1 DNA methylation 5

1.3.2 Histone modifications 6

1.3.3 RNA associated silencing 8

1.4 Long non-coding RNAs 8

1.5 Epigenetic and cancer 11

1.5.1 Epigenetic regulation in human parathyroid tumors 12

2. AIM OF THE WORK 14

3. MATERIAL AND METHODS 15

3.1 Parathyroid samples 15

3.2 Cell line 17

3.3 Primary parathyroid adenoma cells isolation and culture 17

3.4 Antibodies 17

3.5 Western blotting 17

3.6 Cell treatments 18

3.7 Cell transfection and RNA interference 18

3.8 RNA extraction 19

3.9 Quantitative RT-PCR (qRT-PCR) analysis 19

3.9.1 LncRNAs profiling detection in parathyroid samples..... 19

3.9.2 LncRNAs validation in parathyroid samples 19

3.9.3 qRT-PCR analysis in cultured cells 20

3.10 Array Comparative Genomic Hybridization (aCGH) analysis ... 20

3.11 Human Molecular Mechanisms of Cancer Array 21

3.12 Genetic testing 21

3.13 Statystical analysis 22

4. RESULTS 23

4.1 LncRNAs expression profile in human parathyroid tumors 23

4.2 Nine significant lncRNAs are differentially expressed among parathyroid tissues 25

4.3 LncRNAs validation analysis revealed a strong heterogeneity among human parathyroid tumors 29

4.4 Correlation of lncRNAs expression with genetic hallmark of parthyroid carcinomas..... 31

4.5 Identification of genetic alterations in parathyroid adenomas .. 34

4.6 LncRNAs profiling and the genetic background in parathyroid adenomas 37

4.7 Chromosome 11 LOH correlates with HAR1B upregulation 38

4.8 Focus on HAR1B regulation 42

4.9 HAR1B involvement in Wnt/beta-catenin pathway 43

4.10 MEN1 silencing induce HAR1B upregulation in primary parathyroid adenomas cultures 45

4.11 PTH, serum calcium and ionized calcium levels are not influenced by HAR1B lncRNA 47

5. DISCUSSION 48

6. CONCLUSIONS 52

7. BIBLIOGRAPHY 53

8. SITOGRAPHY 63

9. SCIENTIFIC PRODUCTS 64

1. INTRODUCTION

1.1 Parathyroid glands

Parathyroids are small endocrine glands that commonly consist of two pairs of glands generally located closed to the thyroid (Fig. 1). Histologically, each gland is surrounded by a slight capsule covering adipose tissue, vessels and glandular parenchyma. The chief secretory cells are the predominant component of the adult parathyroid glands. The cytoplasm often has numerous lipid bodies and lipofuscin droplets or glycogen granules. The second cell type is the oxyphilic cells, that are singly or scattered among chief cells. They are large cells and their cytoplasmic area is riched in mitochondria. Oxyphil cells of normal parathyroid glands also contain Golgi apparatuses, that are however poorly developed. Parathyroid glands are responsible for the production of the parathormone (PTH), which controls serum calcium levels. PTH is a peptide composed of 84 amino acids that binds PTH1 receptor on target organs. Secretion of PTH is modulated not only by serum calcium, but also phosphorus and vitamin D [1], [2].

PTH effects are related to the target organs. In the bone, PTH binds PTH type I receptors (PTH1R), which is a G-coupled receptor. Its activation involves downstream activation of cAMP/PKA or PKC pathway [3]. PTH acts to increase renal calcium, decrease phosphate reabsorption and activate metabolism of vitamin D. In the intestine, PTH transcriptionally upregulates 1 alpha hydroxylase, leading to increase production of 1,25-dihydroxyvitamin D, which enhances calcium and phosphorus reabsorption.

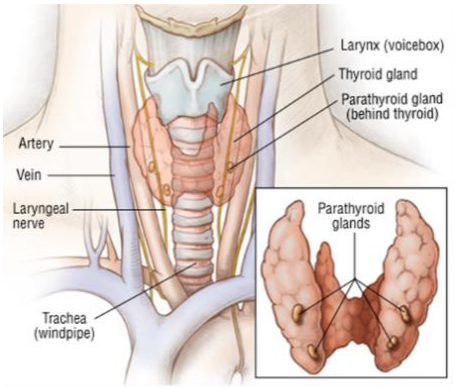

Figure 1. **Anatomy of parathyroid glands** [2]**.**

1.2 Tumors of parathyroid glands

Parathyroid tumor is the third most common endocrine neoplasia after diabetes and thyroid cancer. It has a prevalence in women with a ratio female:male of 3-4:1 and the incidence increased with age. Typically, these tumors are associated to primary hyperparathyroidism (PHPT), an overproduction of PTH with consequent abnormal serum calcium levels [4]. The clinic symptoms range from osteoporosis to mental disorders, ulcers, pancreatitis and kidney stones. Parathyroid tumor usually occurs as a non-familial (sporadic; 90%) or as familial endocrinopathy (10%). The most common parathyroid tumor is adenoma (80-85%), a benign lesion that typically involves a single gland, while atypical adenomas and carcinoma are rarer (1-2%; fig. 2) [5]. PHPT could be caused also by another disorder called hyperplasia (15%). Moreover, there are complex endocrine syndromes, such as multiple endocrine neoplasia 1 (MEN1) and hyperparathyroidism-jaw tumor (HPT-JT) syndrome, that results in PHPT development [6].

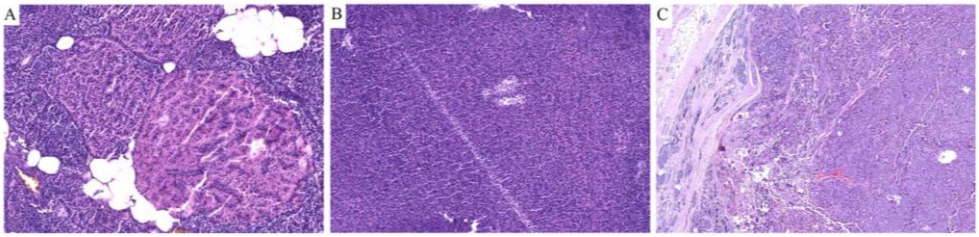

Figure 2. **Histology of parathyroid tumors**. Parathyroid hyperplasia (A), adenoma (B) and carcinoma (C). Hematoxylin-eosin stain (X200 magnification) [5].

1.2.1 Parathyroid adenomas

Most adenomas occur as sporadic lesions. 25-40% of sporadic adenomas are characterized by somatic mutations in the MEN1 gene (Multiple Endocrine Neoplasia 1; locus 11q13.1). This gene codifies for a 67KDa protein, named MENIN, that is ubiquitously expressed and mainly located in the nucleus. MEN1 acts as a tumor suppressor in many tissues thanks to its interaction with several transcription factors [7]. It is involved in many cellular processes including DNA repair, transcriptional regulation and signal transduction [8]. Its target genes are essential for proliferation and development and it cooperates to the recruitment of histone-modifying enzyme [9]–[11]. Overall, MEN1 inactivation results in tumor predisposition (Fig. 3). MEN1 is a syndrome that presents an autosomal dominant pattern of inheritance and, in sporadic cases, a second hit model of tumorigenesis is proposed [12], [13]. Mutation in this gene is the most frequent aberration observed in 30% of sporadic endocrine tumors [14]. Moreover, MEN1 protein is implicated in the apoptosis process since its inactivation causes G_0/G_1 to S phase transition and subsequent cell proliferation [15]. A subset of parathyroid adenomas is mutated for the oncogene cyclin D1/PRAD1 (locus 11q13). Particularly, in 8% of adenomas, this gene undergoes to a rearrangement with PTH gene which controls MEN1 expression [16]. Since parathyroid adenomas are characterized by high levels of PTH, this rearrangement cause cyclin D1 overexpression suggesting its possible

involvement in parathyroid neoplasia [17], [18]. Evidences support the idea that mutations in CDKN1B/p27 inhibitor, β-catenin and POT1 contribute to the pathogenesis of parathyroid adenomas [16]. Moreover, it has been demonstrated that, in parathyroid adenomas, there is a reduction in Calcium Sensing Receptor (CaSR) on the cell surface that affects PTH secretion and cell proliferation [19], [20].

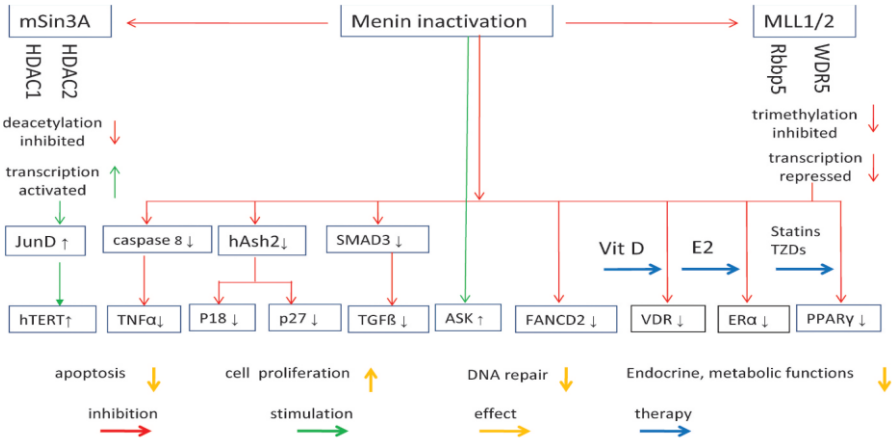

Figure 3. **Schematic representation of modifications resulting from MEN1 mutations** [11].

1.2.2 Parathyroid carcinomas

Parathyroid carcinoma is one of the most aggressive endocrine tumors characterized by a hypersecretion of PTH and serum calcium levels higher than parathyroid adenomas [21], [22]. Rarely, parathyroid carcinomas arise as a consequence of pre-existing adenomas [23]. It is very difficult to diagnose this type of cancer because its histology can be ambiguous and not all carcinomas present the same features. Typically, parathyroid carcinomas are characterized by irregular border, invasion of surrounding tissue, capsular and vascular invasion and metastasis. The best cure is the complete surgical resection [5], [24]. Cell Division Cycle 73 gene (CDC73) is characterized by mutations in more than 70% of sporadic parathyroid

carcinomas [25]–[27]. This gene codifies for a protein, parafibromin, that has a tumor suppressor role in parathyroid tissues by interacting with PAF1 (Polymerase Associated Factor 1), which regulates transcription and histone methylation [28]. Parafibromin prevents cell proliferation by inhibiting c-Myc and cyclin D1 expression [29]. Currently, it is the most specific biomarker for parathyroid carcinoma diagnosis [30]. Moreover, alterations in CaSR and Wnt/β-catenin signaling pathway are involved in parathyroid carcinomas onset [31].

1.3 Epigenetic

Epigenetic is a term referred to alteration of gene activity without modifications in DNA sequence [32]. Epigenetic mechanisms are essential for physiological processes and normal development in mammals [33]. Epigenetic modifications are regulated by different mechanisms that include: DNA methylation, histone modifications and RNA associated silencing (non-coding RNAs) [34]. Failure in these processes can result in signaling pathways alteration and can lead to malignant transformation [35].

1.3.1 DNA methylation

One of the most well-known post-transcriptional modification in eukaryotes is the DNA methylation, a reversible process that contributes to the stability of the genome through chromatin silencing [36]. DNA methylation in mammals typically target cytosine residues at position 5 (5mc) in CpG sites. Specifically, this modification is associated with gene silencing and inhibits the interaction between DNA and transcription factors [37]. This process is catalyzed by a class of DNA methyltransferases enzymes (DNMTs) that transfer a methyl group on 5mc [38], [39]. DNMT1, 3A and 3B are the components of the cellular methylation machinery. DNMT1 is responsible for the maintenance of methylated DNA regions, while DNMT3A and 3B are involved in *de novo* methylation processes [40], [41]. Physiologically,

parental epigenetic imprinting (such as X-chromosome inactivation in female) is controlled by DNA methylation but this mechanism also regulates the expression of non-imprinted genes [42]–[44].

1.3.2 Histone modifications

Histones are the central components of the nucleosome, which is the basic unit of the chromatin. Particularly, histone proteins are assembled to form an octameric core composed by a double pair of H2A, H2B, H3 and H4, surrounded by DNA [45]. Histones modifications are important in gene expression regulation [46]. These proteins can undergo to post-translational modifications such as acetylation, methylation and phosphorilation, at their N-terminal tail, to ensure chromatin accessibility [47], [48]. These modifications can regulate histones interactions but can also recruit histone remodeling complexes [49].

Histone methylation. Compared to other histone modifications, methylation is more stable and is involved in long-term silencing of specific genomic regions [50]. Lysine methylation on H3 histone is the most frequent histone modification and it is highly dynamic. Indeed, this process can promote both transcriptional activation, through H3K4 and H3K36 trimethylation (me3), or inhibition, through H3K27me3 and H3K9me3. Histone lysine methyltransferases (HKMTs) are the enzymes responsible for the histone methylation on lysine residues. [51].

The Polycomb group proteins (PcG) are essential for the maintenance of gene silencing during development. Particularly, they are associated with chromatin remodelling during embryogenesis and tissue differentiation [49], [52], [53]. In mammals, gene silencing involved 2 PcG complexes: Polycomb Repressive Complex 1 and 2 (PRC1 and PRC2, respectively; fig. 4). PRC2, is responsible for H3K27 trimethylation. It is composed by 4 subunit: SUZ12, EED, RABAP48 and EZH2, the catalytic

subunit [54], [55]. PRC1 identifies trimethylated H3K27 and ubiquitinylates histone H2AK119 to inhibit transcriptional elongation. Components of this complex are RING1B, the catalytic subunit, BMI-1, PH1 and CBX [56]. Interestingly, there is a link between histone modifications and DNA methylation [57].

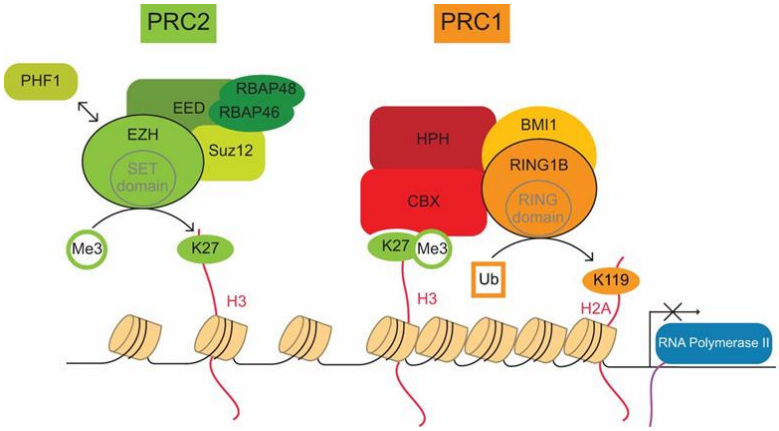

Figure 4. **Schematic representation of PRC complexes and their activity** [58].

Histone acetylation. This modification is a dynamic process, regulated by the opposite action of two classes of enzymes: histone acetyl transferases (HATs) and histone deacetylases (HDACs). HATs promote chromatin activation by adding an acetyl group to a residue of lysine, through the cofactor CoA [59]. Conversely, HDACs remove this residue resulting in chromatin stabilization and transcriptional repression [60], [61].

Histone phosphorylation. Typically, this histones modification occurs on serine, threonine and tyrosine residues in the N-terminal tail [62]. This process is coordinated by kinases and phosphatases enzymes. Kinases are deputies to the transfer of a phosphatase group from ATP to the aminoacidic chain. The recruitment of the enzyme on chromatin is still unknown and probably required interaction with chromatin binding factors [62].

1.3.3 RNA associated silencing

Non-coding RNAs (ncRNAs) are RNA molecules that do not codify for proteins. Recent evidences show that they are important epigenetic regulators [63]. ncRNAs can be subdivided in 2 classes: the short ncRNAs, which include microRNAs (miRNAs), silencing RNAs (siRNAs) and Piwi-interacting RNAs (piRNAs) and the long ncRNAs (lncRNAs; Table 1; [64].

Name	Size	Source	Main functions
siRNA	19-24 bp	Double stranded RNA	Silent transcription gene
miRNA	19-24 bp	pri-miRNA	Silent transcription gene
piRNA	26-31 bp	Long single chain precursor	Transposon repression DNA methylation
lncRNA	>200 bp	Multiple ways	Genomic imprinting X-chromosome inactivation

Table 1. **ncRNAs involved in epigenetic regulation** [65]**.**

1.4 Long non-coding RNAs

Long non-coding RNAs (lncRNAs) are RNA molecules longer than 200 nucleotides, located within nuclear or cytosolic compartment. They are present in different tissues and most of them are expressed in the brain [66]. LncRNAs share similar features with mRNAs, since most of them are transcribed in the 5' to 3' direction by RNA polymerase II and are characterized by a 5'-cap and a 3'-poly(A) tail [67], [68]. LncRNAs can be distinguish in 5 categories: (A) intergenic, (B) bidirectional, (C) intronic, (D) antisense and (E) sense (Fig.5; [69]). Class A is characterized by lncRNAs located 5Kb away from protein-coding genes (e.g. H19, Xist and linc-p21; [70]). LncRNAs that are transcribed in the opposite direction of a protein-conging gene and are generally located 1Kb away from the promoter of the coding gene, belong to class B. Intronic lncRNAs, from class C, start in the intron of a coding gene and do not overlap exons. Antisense lncRNAs, also called Natural Antisense Transcript (NATs), are transcribed in the opposite

direction of protein-coding genes and overlap with the coding sequence while sense lncRNAs overlap with the sense strand and are mainly located in the enhancer region (MALAT1; [71]).

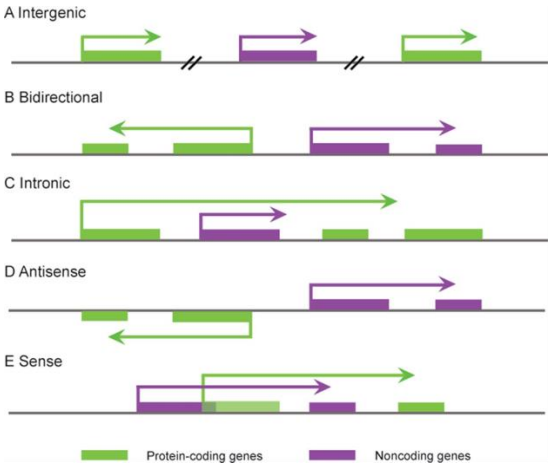

Figure 5. **Classification of lncRNAs according to the genomic location** [72].

LncRNAs are functional molecules. Indeed, they are involved in several processes such as differentiation, development, gene imprinting and antiviral response [73]–[75]. Moreover, some lncRNAs interact directly with DNA, recruit chromatin modifiers, induce chromatin repression and contribute to genes silencing [76]. These data indicate that lncRNAs play an important role as epigenetic regulators, but the molecular mechanisms in which they are involved are still primarily unknown. Furthermore, some lncRNAs are implicated in post-transcriptional regulation such as splicing, protein stability or decoys for microRNAs [77].

Functionally, lncRNAs are extremely heterogeneous. To date, lncRNAs are implicated in 4 mechanisms of action: they can act as (I) signal, (II) guide, (III) decoy and (IV) scaffold (Fig. 6; [78], [79]).

Signal lncRNAs. The majority of lncRNAs show cell-type specificity and are regulated by different stimuli. For these reasons, lncRNAs can act as molecular signals of different biological events. This is the case of

KCNQ1OT1, Air and Xist. Kcnq1ot1 maps on the paternal allele and has been shown to interact with PRC2 and to silence several genes [80]. Similarly, HOTAIR and HOTTIP regulate HOXA genes expression during human development [81]. Spatio-temporal regulation is important also during the stress process. Particularly, lincRNA-p21 and PANDA are activated in response to DNA damage [82].

Decoy lncRNAs. LncRNAs are able to bind proteins by inhibiting their physiological function. In this case they act as decoy molecules for transcription factor or chromatin modifier. TERRA, PANDA and Gas5 lncRNAs belong to this group. Gas5, for example, represses the glucocorticoid receptor by mimiking the DNA motif in the promoter of glucocorticoid-responsive genes. Moreover, it competes for DNA-binding domain on the same receptor [83]. LncRNAs can function as decoy for microRNAs. This is the case of MALAT1, located at the nuclear speckles, whose absence induce a modification of alternative splicing of some pre-miRNAs [84].

Guides lncRNAs. This class of lncRNAs interact with ribonucleoproteins complexes and direct them to a specific target region. Some of them act in *cis* (Xist, Air, HOTTIP; [85]), while others in *trans* (HOTAIR, LincRNA-p21 and Jpx; [86]).

Scaffold lncRNAs. This class of lncRNAs is the most functionally complex. Indeed, these lncRNAs are characterized by distinct domains that bind different molecules. HOTAIR belong to these class of lncRNAs. Particularly, it binds the PRC2 complex in the 5' end, promoting transcriptional inhibition. In addition, its 3' end binds RE1 Silencing Transcription Factor (REST) that antagonized PRC2 activity [87]. Scaffold lncRNAs class include also TERC and ANRIL [88].

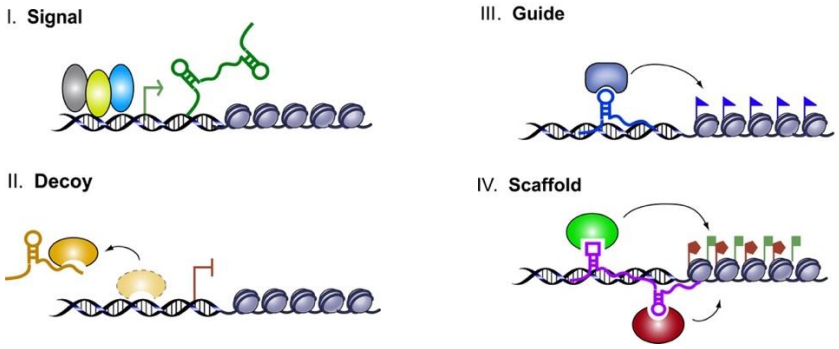

Figure 6. **Mechanisms of lncRNAs activity** [79].

1.5 Epigenetic and cancer

Many evidences highlight a correlation between epigenetic and cancer. Epigenetic alterations promote cancer development and contribute to cancer progression [89], [90]. Recent studies demonstrate that alterations in the epigenetic regulation are key events in cancer onset [91]. Tumors are characterized by alterations in DNA methylation and histone modifications that can lead to the repression of tumor suppressor genes. Furthermore, the epigenetic abnormalities can also promote the activation of several oncogenes [34], [89]. There are two processes of DNA methylation that occur in cancer cells: the demethylation process and *de novo* CpG island methylation. By 5-azacytidine (5-AZA), a demethylating compound, it has been shown that methylation has an important role in tumorigenesis. Indeed, after 5-AZA tumor cells treatment, some *de novo* methylated genes are upregulated and tumor cells lose their cancer properties [92]. Interestingly, most of these genes are targets of the Polycomb Repressive Complex 2 [93]. Post-translational modifications of histones have been widely related to cancer. These modifications induce chromatin accessibility and impact on gene expression pattern [94]. Recent evidences show that lncRNAs are involved in many biological processes, including cancer. Particularly, the role of each lncRNA is related to the cellular localization. Nuclear lncRNAs control

the epigenetic condition of several genes by recruiting chromatin modifier or epigenetic regulators on specific loci [95]. LncRNAs deregulation is implicated in different step of tumorigenesis among which the resistance to apoptosis, cell proliferation, angiogenesis and metastasis [96]. Moreover, they are directly involved in epigenetic changes which include histone modifications, chromatin remodelling and DNA methylation (Table 2). For example, the lncRNA ANRIL is altered in 50-60% of human tumors and the chromatin modifier HOTAIR is upregulated in breast cancer [97]. Evidences highlight an altered expression of lncRNAs in endocrine malignancies. Several lncRNAs are downregulated in thyroid cancer, including NAMA and AK023948 [98].

Name	Cancer	Mechanism
ANRIL	High expression linked to poor outcome in prostate and gastric cancer.	Interacts with CBX7 and PRC2 to silence the INK4b/ARF/INK4a locus.
CCAT1-L	Upregulated in human colorectal cancers	Regulates long-range chromatin interactions to activate the transcription of the MYC locus.
DACOR1	Downregulated in colon tumors.	Interacts with and inhibits the DNA methyltransferase DNMT1.
ecCEBPA	Shows inverse correlation with CEBPA in leukaemia cell lines.	Interacts with DNMT1 and prevents CEBPA locus methylation.
FAL1	Frequently amplified in human cancers.	Interacts with PRC1 to silence the CKDN1A locus.
H19	Promotes oncogenesis in different cancer types.	Interacts with SAHH inhibiting the DNMT3Bdependent DNA methylation at different genetic loci.
HOTAIR	Overexpressed in liver, metastatic breast, lung and pancreatic tumors.	Interacts with PRC2 and LSD1 to silence genes.
HOXA11-AS	Acts as oncogene or tumor suppressor depending on the cellular context.	Interacts with PRC2, LSD1 and DNMT1 to silence genes
LED	Downregulated in p53 wild-type leukaemia.	Promotes CDKN1A transcription by acting as enhancer RNA.
LINC-PINT	Downregulated in colorectal cancer	Interacts with PRC2 to silence genes.

Table 2. **List of lncRNAs with deregulated function in cancer** [95].

1.5.1 Epigenetic regulation in human parathyroid tumors

Recent studies demonstrated that parathyroid tumors are characterized by epigenetic alterations. Particularly, DNA methylation and chromatin remodelling complexes are deregulated in parathyroid tumors. Genetic alterations influence the epigenetic status of parathyroid cells through the

MEN1 and parafibromin interaction with chromatin modifiers [99]. The epigenetic profile of parathyroid carcinomas has been deeply investigated. Several studies described hypermethylation of CpG islands and the impairment of PRC2 components EZH2 and BMI1 [100]. Different genes are hypermethylated in CDC73-mutated parathyroid carcinoma: *APC*, *SFRP1*, an antagonist of the Wnt pathway, *CDKN2A/B*, involved in cell cycle control, *PYCARD*, involved in apoptosis, *HOXC11* and *HIC1* transcription factors [101]. Specifically, *HIC1* repression is related to H3K27me3 modification induced by EZH2 [102]. Despite there are no evidences of lncRNAs alterations in parathyroid tumors, recent studies highlights the important role of microRNAs (miRNAs) in parathyroid epigenetic regulation [103], [104]. Particularly, a general miRNAs downregulation in parathyroid carcinomas compared to normal glands was observed. Some of these miRNAs are downregulated also in the distant metastasis of parathyroid carcinomas. This is the case of mir-296-5p which is downregulated in lung metastasis [103]. Our laboratory demonstrated that parathyroid tumors are characterized by a deregulation of two clusters, the C19MC and miR-371-373 [103]. Recently, we also showed that miR-372 is aberrantly overexpressed in a set of parathyroid adenomas, atypical adenomas and carcinomas. Specifically, we demonstrated that miR-372 is able to inhibit p21 and LATS2 in primary parathyroid adenomas cultures. Moreover, our findings show that miR-372 is involved in Wnt pathway inhibition and positively correlated with PTH serum levels [105].

2. AIM OF THE WORK

The aim of this work is to shed light on the lncRNAs alterations in human parathyroid tumors to identify a ‘molecular signature’ able to distinguish among parathyroid histotypes. Moreover, we aim to analyze the importance of epigenetic alterations occurring in parathyroid tumors to discover new potential diagnostic biomarkers.

3. MATERIAL AND METHODS

3.1 Parathyroid samples

For lncRNAs profiling we analyzed two patient's set. The first series consisted in 4 parathyroid carcinomas (PCas), 12 parathyroid adenomas (PAds) and 2 normal parathyroid glands (PaNs), incidentally removed from normocalcemic patients having undergone thyroid surgery. Specimens from PCas were sampled from the central portion of the tumors to avoid the contamination of parathyroid tissue with adjacent non-parathyroid tissue. The second set, used for data validation, was composed by 7 PCas, 26 PAds, 6 atypical adenomas (aPAds) and 4 PaNs. All samples were from frozen tissues except for formalin-fixed paraffin embedded (FFPE) PaNs from the second set. Histologic classification of PCas and aPAds was established according to WHO published guidelines (Bondeson et al., 2004). In all patients, fasting serum total and ionized calcium and phosphate were measured by a multichannel autoanalyzer. Intact PTH was determined by a chemiluminescent immunoassay (Nichols Advantage, Nichols Institute Diagnostics, San Clemente, CA, USA) in order to diagnose primary hyperparathyroidism. Clinical and biochemical features are reported in Table 3. Written informed consent was obtained from all the participants.

Sample	Gender	Age at diagnosis of PHPT	Serum calcium (mg/dl)	Ionized calcium (mmol/l)	PTH levels (pg/ml)
PAd 1	F	41	11.4	1.43	256
PAd 2	F	63	12.8	n.a.	181
PAd 3	F	54	10.4	1.3	166
PAd 4	M	56	12.1	1.56	216
PAd 5	F	52	11.6	1.46	125
PAd 6	F	65	9.6	1.31	90.5
PAd 7	M	61	12.2	1.6	280
PAd 8	F	47	10.1	1.33	172
PAd 9	F	65	10.3	1.42	95
PAd 10	F	64	12.1	1.47	592
PAd 11	M	n.a.	n.a.	n.a.	n.a.
PAd 12	F	79	11.4	1.43	108
PAd 13	F	61	10.5	1.52	166
PAd 14	M	38	9.4	1.42	159
PAd 15	M	76	11.9	1.73	384
PAd 16	F	35	12.2	1.89	1410
PAd 17	F	68	9.6	1.38	586
PAd 18	F	63	14.6	1.71	231.8
PAd 19	F	72	11.2	1.53	115
PAd 20	F	74	10.8	1.32	498
PAd 21	F	80	11.6	1.45	178
PAd 22	F	78	11.2	1.37	153
PAd 23	F	76	13.7	1.94	382
PAd 24	F	67	12.1	1.58	292
PAd 25	M	59	12.2	1.53	214
PAd 26	F	29	11.1	1.48	408
aPAd 1	F	61	12.1	1.72	872
aPAd 2	M	80	13.2	1.97	353
aPAd 3	M	61	13.7	1.48	1151
aPAd 4	M	83	14	1.63	419
aPAd 5	n.a.	n.a.	16.2	2.35	953
aPAd 6	n.a.	n.a.	12.2	1.84	738
PCa 1	F	37	13	1.8	660
PCa 2	F	55	16.1	1.6	293
PCa 3	F	54	17.6	1.93	940
PCa 4	F	26	11.5	1.5	106
PCa 5	M	64	13.9	2.13	690
PCa 6	F	37	13	1.93	660
PCa 7	F	55	16.1	2.1	293
PCa 8	n.a.	n.a.	11.2	1.58	63
PCa 9	n.a.	n.a.	12.2	1.56	96
PCa 10	n.a.	n.a.	14.4	1.94	2058
PCa 11	n.a.	n.a.	11.4	1.54	167

Table 3. **Clinical and biochemical features of patients analyzed for lncRNAs profile and validation analysis.**

3.2 Cell line

The HEK293 cell line (Human embryonic kidney; AmericanType Culture Collection) used for transient silencing was grown in DMEM (1X) + Glutamax^{TM}-I supplemented with 10% FBS, 100 U/liter penicillin/streptomycin and 1mM sodium pyruvate (all from Gibco). All cells were cultured at 37°C in a humidified atmosphere of 5% CO_2/air.

3.3 Primary parathyroid adenoma cells isolation and culture

Primary cells were isolated directly from patient's sample after surgery resection. Samples obtained from tumor were disaggregated mechanically and enzymatically using Collagenase type I (2mg/ml) and replaced at 37°C for 90 minutes. Then, cells were filtered in 100µM Cell Strainer and pelleted by centrifugation for 5 minutes at 1600rpm. After that, primary cells were seeded in DMEM supplemented with 10% FBS (Gibco).

3.4 Antibodies

For Western blotting the following antibodies were used: MEN1 (EPR3986) rabbit (ab92443; Abcam); EZH2 (D2C9) rabbit (5246; Cell Signaling Technology); EED (H-300) rabbit (sc-28701; Santa Cruz Biotechnology); trimethyl-histone H3 (Lys27) rabbit (07-449, Sigma-Aldrich); β-tubulin mouse (T8328, Sigma); HRP-linked anti-rabbit and anti-mouse (BioRad).

3.5 Western blotting

Confluent cells were lysed by boiling in RIPA buffer (50-mM Tris-HCl, pH 7.4, 150-mM NaCl, 1% Triton X-100, 0.5% deoxycholic acid, 0.1% SDS, 150-mM NaCl, 2mM-EDTA, 50mM-NaF) supplemented with 1X complete protease and phosphatase inhibitors cocktail (Roche). For tissues, samples were put in 1ml Trizol (Ambion) and mechanically disrupted using TissueLyser (Qiagen), following the manufacturer's protocol. After lysis, cells were

sonicated and protein concentration was estimated using the BCA Protein Assay Kit (Pierce). Equal amounts of proteins were loaded on gels, separated by SDS-PAGE and transferred to a nitrocellulose membrane (BioRad). After incubation with primary and HRP-linked secondary antibodies, specific bindings were detected by a chemiluminescence system (GE Healthcare) using iBright FL1000 imaging system (ThermoFisher Scientific).

3.6 Cell treatments

5-Azacytidine (320-67-2; Sigma-Aldrich) and Tazemetostat (EPZ-6438; Selleckchem) were dissolved in CH_3COOH and dimethyl sulfoxide (DMSO), respectively. Before any treatment, HEK293 cells were seeded into 6-well culture plate at a density of 3 x 10^5 cells/well and cultured overnight in complete medium. Cells were treated with 5, 7 and 10 µM 5-azacytidine (for 48h) or vehicle only. Fresh medium containing the drug was added daily. For Tazemetostat (TAZ) treatment, cells were cultured with 1µM TAZ, for 48h. DMSO was used as negative control.

3.7 Cell transfection and RNA interference

To perform RNA interference, HEK293 cells were seeded (3 x 10^5 cells/well) in 6-well plate. Cells were transfected with HAR1B siRNA (Hs02_00378868; Sigma-Aldrich), MEN1 siRNA (Hs01_00211239; Sigma-Aldrich) or control siRNA (SIC001; Sigma-Aldrich), for 5 hours. Transfection was performed using Lipofectamine 3000 (Invitrogen) in Opti-MEM (Gibco), in accordance with the manufacturer's instruction. After 48 hours, transfected cells were validated for target gene knockdown by qRT-PCR.

3.8 RNA extraction

All samples from frozen tissues were processed with TissueLyser (Qiagen) and total RNA was purified using Triazol reagent (Invitrogen). For FFPE samples and cultured cells, RNA was extracted using MasterPure™ RNA purification kit (Epicentre Biotechnologies). All RNA was quantified by spectrophotometry at 260 nm (NanoDrop ND-1000 Uv/Vis, Thermo Scientif, Whaltham, MA, USA). DNA contamination was removed by DNAse I Amplification Grade (Invitrogen) treatment.

3.9 Quantitative RT-PCR (qRT-PCR) analysis

3.9.1 LncRNAs profiling detection in parathyroid samples

For lncRNAs profiling detection, 1µg of total RNA was reverse-transcribed using cDNA synthesis kit (System Biosciences). LncRNAs quantification was performed with Human LncProfilers™ qPCR Array kit (RA900-A1, System Biosciences) and Power SYBR Green® PCR Master Mix (4367659; Applied Biosystems), according to the manufacturer's instructions. This array contains assays for 90 lncRNAs, 5 endogenous reference RNAs as normalization signal and a negative control (Fig. 7A). LncRNAs with non-specific melting curve were excluded from analysis. For qRT-PCR analysis, Ct data were normalized with the GeNorm algorithm using RNU43 and mammary U6 housekeeping genes. Expression data were then median normalized and log2 transformed.

3.9.2 LncRNAs validation in parathyroid samples

Data validation was performed for significant lncRNAs using the second series of patients and TaqMan chemistry. 500ng of total RNA were reverse transcribed using SuperScript® IV Reverse Transcriptase (18090010; Invitrogen) and the High-Capacity cDNA Reverse Transcription Kit (Thermo Fisher Scientific), following the protocol thermal cycling. DNA contamination

was removed by DNase I Amplification Grade (18068-015, Invitrogen) treatment. The following gene expression assays (all from Thermo Fisher Scientific) were used: AXIN2 (Hs00610344_m1); β-CATENIN (CTNNB1; Hs00355045_m1); CADHERIN 1 (CDH1; Hs01023894_m1); CDKN1A/p21 (Hs00355782_m1); EED (Hs00537777_m1); EZH2 (Hs00544830_m1); HAR1B (Hs03299152_m1); HOXA3as (Hs00940777_m1); HOXA6as (Hs03296494_m1); KCNQ1OT1 (Hs03665990_s1); MEG3 (Hs00292028_m1); MEN1 (Hs00365720_m1); NEAT1 (Hs01008264_s1); SNHG6 (Hs00417251_m1) and WT1-as (Hs04406300_m1). BC200/BCYRN1, a custom assay, designed with Primer Express 3.0.1 software (Forward: 5'-GGTGGCTCACGCCTGTAATC-3'; Reverse: 5'-ACTCCTGGGCTCAAGCTATCC-3'; Probe: 5'-CTCAGGGAGGCTAAGAG-3'; amplicon length: 70bp). For any gene, the expression level was normalized to the housekeeping gene encoding *18S*. Expression data were then PaNs median normalized and log2 transformed.

3.9.3 qRT-PCR analysis in cultured cells

For cultured cells, 1 µg of total RNA was reverse transcribed using the MultiScribe® Reverse Transcriptase (50 U/µl; Thermo Fisher Scientific) and the High-Capacity cDNA Reverse Transcription Kit (Thermo Fisher Scientific), following the protocol thermal cycling. mRNA level was normalized to B2M housekeeping gene. Other reagents and TaqMan probes were the same as described for tissue samples.

All qRT-PCRs were performed using ABI Prism 7900HT instrument (Thermo Fisher Scientific).

3.10 Array Comparative Genomic Hybridization (aCGH) analysis

Genomic DNA of 24 PAds was isolated using Trizol reagent (Invitrogen). Array-CGH analysis was performed using 60 mer oligonucleotide probe technology (SurePrint G3 Human CGH 8 x 60K, Agilent Technologies, Santa

Clara, CA, USA), according to the manufacturer instructions. Agilent Feature Extraction and Cytogenomics 3.0.4.1, with the ADM-2 algorithm (Agilent Technologies, Santa Clara, CA, USA) were used to generate and analyze data. To improve the precision of the results, the Diploid Peak Centralization algorithm was applied. The filter of aberration was set to identify a minimum of five consecutive probes/regions, and the minimum absolute average log ratio (MAALR) was ± 0.25. To individualize low level of mosaicism, a second analysis was run with a MAALR of ± 0.15 (again with a minimum number of five probes/regions). Only copy number variants not already reported in the public database of genomic variants (http://projects.tcag.ca/variation/) were listed. Genomic coordinates agree to the build 37 assembly (March 2009) of the Human Genome Reference consortium (GRch37/hg19).

3.11 Human Molecular Mechanisms of Cancer Array

The TaqMan™ Array, Human Molecular Mechanisms of Cancer plate (4418806, Fast-96 well, Thermo Fischer Scientifc) is a commercial array that allow to investigate the expression of 92 genes associated with the most important molecular mechanisms of cancer. Four endogenous control genes are included (Fig. 16B). Analysis was performed loading 10ng/well of cDNA from HEK293 cells transfected with siHAR1B and control siRNA, according to the manufacturer's instructions. TaqMan® Fast Advanced MasterMix was used (Applied Biosystems). qRT-PCR analysis was performed on StepOnePlus® RT-PCR detection System (Applied Biosystems).

3.12 Genetic testing

Genomic DNA was extracted from 7 parathyroid carcinomas using standard methods. The entire coding sequence of the CDC73 gene, including the exon-intron boundaries, was sequenced by PCR amplification and direct all the 17 exons (16 amplicons) were sequenced as previously described [106]. Briefly, the entire coding sequence of CDC73 (17 exons) was performed on

100 ng of DNA. Amplifications were carried out in a 25 µl reaction volume containing 10X PCR Buffer, 0.25 nM dNTPs, 20 pmol of each primer and 1 U HotMaster Taq (all from Eppendorf). PCR products were purified using the GFX™ PCR and Band Purification Kit (GE Healthcare). The BigDye Terminator Cycle Sequencing Kit v.1.1 (Applied Biosystems) and ABI 3100 capillary sequencer (Applied Biosystems) were used. Data were analyzed using the Sequencing Analysis software v.3.7. Reactions without DNA were used as PCR controls. No other carcinomas samples were available at the time of the study.

3.13 Statystical analysis

For SYBR Green lncRNAs discovery, only transcripts with a Ct value < 35 in at least half plus one sample were considered for statistical analysis. For unsupervised hierarchical clustering, “ComplexHeatmap” R package (RStudio Team 2015; version 3.2.4) was used. Principal Component Analysis representation was developed by “Corrplot” and “PCA3d” packages on RStudio platform. SAM packages on RStudio (samr) was used to identify significant changes in lncRNAs expression levels. All lncRNAs with a fold change (FC) ≤ 0.5 and ≥ 2 (data not log2 transformed) and a q-value < 5% were considered statistically significant. For the validation set, we considered as expressed each lncRNA with a Ct value <40. Statistical analysis was performed using GraphPad Prism 7 software. Parametric one-way ANOVA adjusted for multiple testing using the Dunn’s method was performed. A Student’s two-tailed Mann-Whitney U- test was used to determine statistical significance between 2 groups. The significance level was set at $P < 0.05$.

4. RESULTS

4.1 LncRNAs expression profile in human parathyroid tumors

In order to study lncRNAs expression in human parathyroid tissues we profiled 90 lncRNAs (Fig. 7A) in an initial set of 4 parathyroid carcinomas (PCas), 12 parathyroid adenomas (PAds) and 2 normal parathyroid glands (PaNs).

The unsupervised analysis (Fig. 7B) distributed samples in two main clusters. Normal parathyroids and carcinomas were distinctly separated. In particular, PaNs overexpressed most of the lncRNAs analyzed. Interestingly, the clustering evidenced different subgroups of adenoma samples, indicating the heterogeneity of lncRNAs expression in PAds. Using Principal Component Analysis (PCA; fig. 7C), PaNs and PCas clustered separately while PAds were scattered among the two components, consistently with what we observed with hierarchical clustering.

A

Human LncProfiler qPCR Array

	1	2	3	4	5	6	7	8	9	10	11	12
A	21A	7SK	7SL	Air	AK023948	Alpha 280	Alpha 250	ANRIL	anti-NOS2A	antiPeg11	BACE1AS family	BC200
B	CAR Intergenic 10	DHFR upstream transcript family	Dio3os family	DISC2 family	DLG2AS	E2F4 antisense	EgoA	EGO B	Emx2os	Evf1 and EVF2	GAS5-family	Gomafu
C	H19	H19 antisense	H19 upstream conserved 1&2	HAR1A	HAR1B	HOTAIR	HOTAIRM1	HOTTIP	Hoxa11as	HOXA3as	HOXA6as	HULC
D	IGF2AS family	IPW	Jpx	Kcnq1ot1	KRASP1	L1PA16	LncRNA-p21	Lnc-RoR	Lnc-SFMBT2	Lnc-VLDLR	LOC-285194	LUST
E	Malat1	mascRNA	MEG3 family	MEG9	MER11C	ncR-uPAR	NDM29	NEAT1	Nespas	NRON	NTT	p53 mRNA
F	PCGEM1	PR anti-sense transcripts	PRINS	PSF inhibiting RNA	PTENP1	RNCR3	SAF	SCA8	snaR	SNHG1	SNHG3	SNHG4
G	SNHG5	SNHG6	Sox2ot	SRA	ST7OT	TEA ncRNAs family	Tmevpg1	TncRNA	Tsix	TUG1 family	UCA1	UM9-5
H	WT1-AS	Xist	Y RNA-1	Zeb2NAT	Zfas1	Zfhx2as	18S rRNA	RNU43	GAPDH	LAMIN A/C	U6	No assay control
							Control reference Assays					

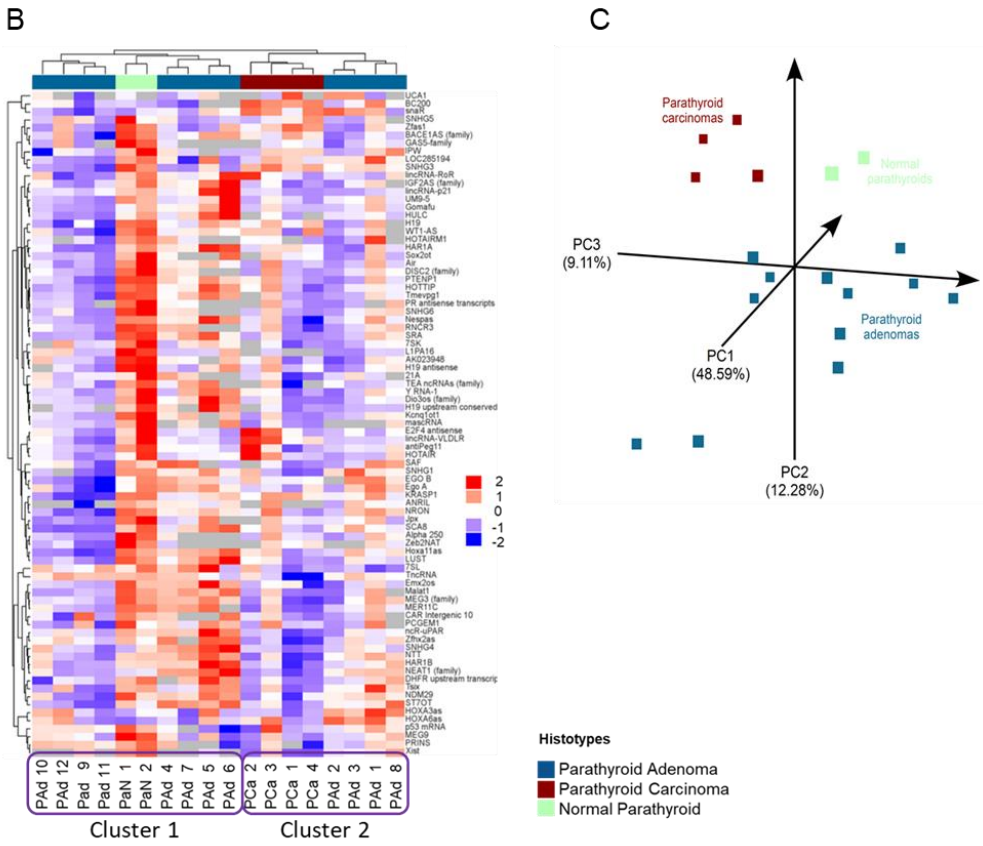

Figure 7. **LncRNAs expression profile in human parathyroid tumors.** (A) Representation of the Human LncRNA Profiler qPCR Array (Human) plate. It included assays for 90 lncRNAs, 5 control references and one negative control. (B) Unsupervised Hierarchical Clustering of differentially expressed lncRNAs in 3

parathyroid tissues. Pearson correlation metric, complete linkage algorithm was performed. Gray squares indicated undetermined lncRNAs expression (Ct ≥ 35). (C) Principal Component Analysis (PCA) showed a graphical distribution of samples according to the first 3 principal components. Blue squares = PAds, red squares = PCas, green squares = PaNs. The first three PCA-components explained 69.98% of the variance in the dataset (48.59%, 12.28% and 9.11% for PC1, PC2 and PC3, respectively).

4.2 Nine significant lncRNAs are differentially expressed among parathyroid tissues

To identify differences in lncRNAs expression between the 3 parathyroid histotypes SAM significance analysis was performed (Fig. 8; table 4). Nine lncRNAs were identified as differentially expressed between parathyroid tissues (q-value < 0.05; table 5). Specifically, KCNQ1OT1 and SNHG6 were enriched in PaNs, HAR1B, HOXA3as, MEG3 and NEAT1 expression characterized PAds, whereas BC200 and HOXA6as were significantly upregulated in PCas compared to PaNs. WT1-AS is upregulated both in PaNs and PCas.

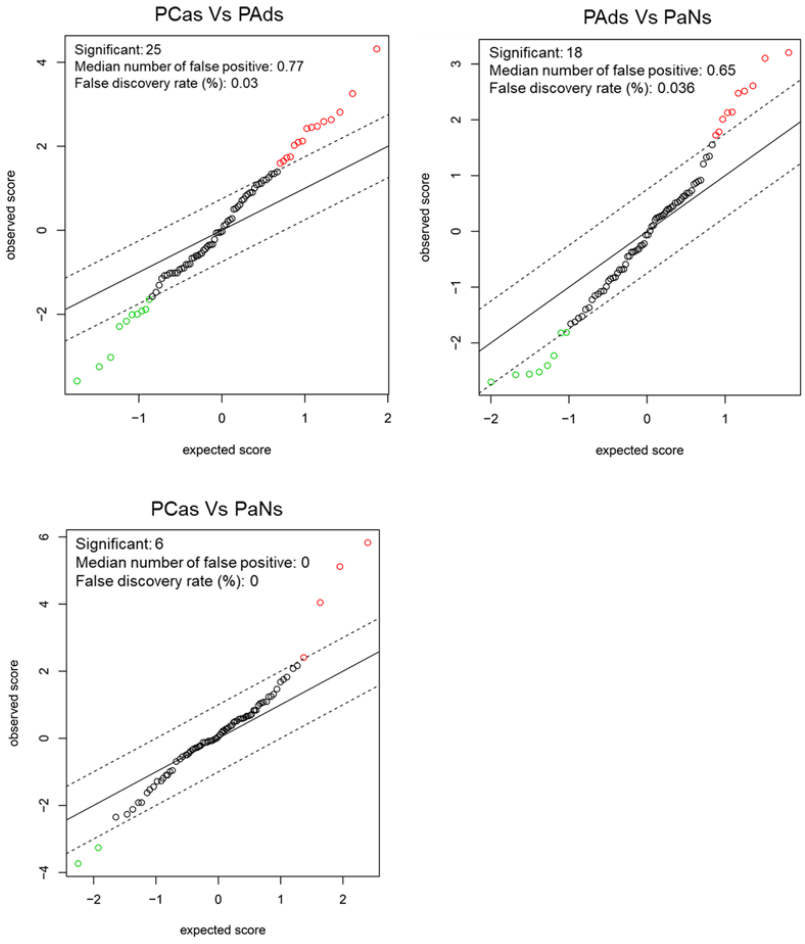

Figure 8. **Significance Analysis of Microarray plots comparing human parathyroid tissue classes.** The two parallel dashed lines were the cut-off threshold specified by the false discovery rate (FDR) and the total number of upregulated (red dots) and downregulated (green dots) genes were given for each plot (n=25, n=18, n=6, respectively). Black points denoted genes that do not show altered expression. FDR < 0.05; q-value < 0.10; fold change (FC) ≥ 2 and ≤ 0.5 (data not log transformed).

	PAds / PaNs			PCas / PaNs			PCas / PAds		
Gene Name	**Score-d**	**FC**	**q-value**	**Score-d**	**FC**	**q-value**	**Score-d**	**FC**	**q-value**
21A	0.43	0.29	51.12	-0.22	0.17	73.00	-1.65	0.60	3.08
7SK	-1.40	0.14	13.01	-1.92	0.07	14.91	-0.39	0.51	24.03
7SL	0.40	0.63	51.12	0.28	0.33	58.59	-0.22	0.52	31.54
AIR	-1.66	0.14	8.49	-0.55	0.17	73.00	1.12	1.18	7.50
AK023948	-0.59	0.26	33.29	-0.12	0.25	73.00	0.52	0.98	19.59
Alpha 250	-1.52	0.16	8.49	-0.28	0.21	73.00	1.20	1.31	6.43
ANRIL	0.63	0.60	49.32	1.82	1.17	12.23	2.02	1.95	0.00
antiPEG11	-0.85	0.21	23.97	0.23	0.81	58.59	1.19	3.88	6.43
BACE1-AS	-0.45	0.31	42.49	0.66	0.41	46.39	1.75	1.32	1.75
BC200	1.78	1.54	4.07	5.12	5.58	0.00	3.25	3.63	0.00
CAR-intergenic-10	0.68	0.62	48.80	0.50	0.33	54.07	-0.61	0.53	22.44
DHFR-upstream-transcripts	0.28	0.57	52.39	-1.10	0.18	38.55	-1.31	0.31	11.28
DIO3OS	-0.82	0.29	23.97	-1.62	0.10	22.09	-1.02	0.33	15.12
DISC2	-1.82	0.16	3.61	-0.96	0.16	54.07	-0.05	1.05	35.73
E2F4-antisense	-0.69	0.17	29.43	0.98	0.92	31.81	2.63	5.30	0.00
EGO-B	0.40	0.65	51.12	1.24	0.52	25.30	0.90	0.81	11.28
EGO-A	0.73	0.68	48.80	0.67	0.36	46.39	-0.05	0.53	35.73
EMX2-OS	0.85	0.53	37.38	0.32	0.32	58.59	-0.34	0.61	24.82
GAS5	-0.35	0.27	43.37	0.39	0.29	54.07	0.90	1.08	11.28
Gomafu	0.69	5.95	48.80	1.04	0.41	29.45	-0.33	0.07	24.82
H19	-1.08	0.24	19.72	0.59	0.35	54.07	2.12	1.43	0.00
H19-antisense	-2.56	0.12	0.00	-1.28	0.15	31.81	1.65	1.24	3.21
H19 upstream conserved 1 & 2	-0.33	0.40	43.37	-0.69	0.13	71.57	-0.82	0.33	16.91
HAR1A	1.33	0.70	12.05	1.68	0.62	14.91	1.35	0.90	6.43
HAR1B	2.14	1.36	0.00	0.71	0.36	46.39	-2.16	0.26	0.00
HOTAIR	-0.26	0.23	48.80	1.06	1.18	29.45	2.59	5.14	0.00
HOTAIRM1	2.01	0.62	0.00	1.75	0.55	12.23	0.11	0.89	33.19
HOTTIP	-0.69	0.34	29.43	0.00	0.30	73.00	0.71	0.89	15.12
HOXA11-AS	0.11	0.47	61.04	0.63	0.35	54.07	0.50	0.75	19.59
HOXA3as	2.13	2.18	0.00	2.41	0.75	0.00	-0.91	0.34	15.12
HOXA6as	2.61	3.51	0.00	5.83	3.00	0.00	0.25	0.85	29.30
HULC	0.58	1.32	49.32	0.59	0.34	54.07	-0.48	0.26	24.03
IGF2-AS	0.51	0.69	51.12	-0.23	0.21	73.00	-1.02	0.31	15.12
IPW	-0.37	0.23	43.37	0.51	0.31	54.07	1.26	1.33	6.43
JPX	-2.57	0.07	0.00	-2.12	0.08	12.23	0.86	1.11	11.28
KCNQ1OT1	-2.23	0.12	0.00	-2.26	0.08	7.95	-1.15	0.67	15.12
KRASP1	-0.84	0.27	23.97	1.09	0.50	29.45	2.45	1.85	0.00
L1PA16	-2.70	0.06	0.00	-3.73	0.04	0.00	-0.35	0.71	24.82
lincRNA-p21	0.45	2.13	51.12	-0.50	0.22	73.00	-0.90	0.10	16.91
lincRNA-RoR	0.24	0.51	52.39	0.83	0.79	46.39	1.10	1.54	7.50
lincRNA-VLDLR	-1.55	0.11	8.49	1.25	0.73	25.30	4.32	6.94	0.00
LOC285194	-0.22	0.44	48.80	0.83	0.41	46.39	1.01	0.94	9.38
LUST	-0.25	0.42	48.80	-0.28	0.22	73.00	-0.03	0.53	35.73
MALAT1	-0.37	0.37	43.37	-1.10	0.16	38.55	-1.02	0.43	15.12
mascRNA	-0.99	0.20	21.05	-1.27	0.09	31.81	-1.48	0.47	7.50
MEG3	-0.07	0.37	58.06	-1.44	0.14	29.45	-2.29	0.37	0.00
MEG9	-0.89	0.19	23.97	-1.19	0.14	31.81	-0.06	0.74	35.73
MER11C	0.92	0.47	37.38	-0.39	0.24	73.00	-1.88	0.52	1.75
ncR-uPAR	1.55	1.12	8.49	0.18	0.28	58.95	-2.00	0.25	1.75

	PAds / PaNs			PCas / PaNs			PCas / PAds		
Gene Name	**Score-d**	**FC**	**q-value**	**Score-d**	**FC**	**q-value**	**Score-d**	**FC**	**q-value**
NDM29	0.64	0.48	49.32	-0.08	0.22	73.00	-1.08	0.46	15.12
NEAT1	3.10	3.42	0.00	1.47	0.42	18.71	-3.25	0.12	0.00
NESPAS	0.25	0.50	52.39	-0.45	0.25	73.00	-1.07	0.50	15.12
NRON	-0.68	0.29	29.43	-0.02	0.35	73.00	0.81	1.21	11.93
NTT	2.48	1.02	0.00	0.04	0.32	63.34	-3.03	0.32	0.00
p53-mRNA	0.20	0.41	53.38	0.47	0.54	54.07	0.28	1.33	29.30
PCGEM1	0.29	0.42	52.39	0.61	0.38	54.07	0.61	0.91	18.95
PR-antisense-transcripts	-2.41	0.12	0.00	-1.53	0.15	25.30	0.74	1.29	15.12
PRINS	0.52	0.49	49.32	-0.34	0.27	73.00	-0.81	0.55	16.91
PTENP1	-1.37	0.25	13.01	-0.04	0.26	73.00	1.60	1.04	3.21
RNCR3	0.26	0.33	52.39	-0.12	0.26	73.00	-0.80	0.81	16.91
SAF	1.35	0.82	12.05	1.08	0.36	29.45	-0.67	0.44	22.44
SCA8	-0.06	0.44	58.06	0.57	0.31	54.07	0.56	0.71	18.95
snaR	1.72	2.21	4.07	4.05	4.95	0.00	2.09	2.24	0.00
SNHG1	0.09	0.52	61.04	-0.32	0.27	73.00	-0.65	0.51	22.44
SNHG3	-0.32	0.29	43.37	2.08	0.67	9.94	2.81	2.29	0.00
SNHG4	3.20	1.74	0.00	2.16	0.61	9.94	-1.58	0.35	6.43
SNHG5	-0.45	0.13	42.49	0.22	0.19	58.59	1.08	1.46	7.50
SNHG6	-2.52	0.10	0.00	-3.26	0.08	0.00	-0.55	0.81	22.44
SOX2-OT	-1.23	0.13	16.27	-0.25	0.14	73.00	1.39	1.03	6.43
SRA	-1.07	0.27	19.72	-2.35	0.15	7.95	-0.61	0.53	22.44
ST7OT	1.21	1.58	19.72	0.84	0.44	46.39	-0.94	0.28	15.12
TEA-ncRNAs	0.32	0.40	52.39	-0.07	0.34	73.00	-0.57	0.83	22.44
Tmevpg1	-1.15	0.28	16.27	-0.99	0.21	54.07	0.22	0.74	31.54
TncRNA	0.87	0.69	37.38	-0.62	0.25	73.00	-2.01	0.36	1.75
TSIX	0.90	0.78	37.38	0.27	0.33	58.59	-1.02	0.42	15.12
UCA1	0.55	1.12	49.32	1.31	1.76	25.30	1.34	1.57	6.43
UM9-5	0.01	1.52	61.04	-0.50	0.20	73.00	-0.44	0.13	24.03
WT1-AS	-1.81	0.14	3.61	-0.08	0.32	73.00	1.73	2.31	1.75
XIST	-0.75	0.24	29.43	-1.91	0.10	14.91	-1.92	0.43	1.75
Y RNA-1	0.36	0.38	51.12	0.36	0.27	54.07	0.14	0.71	33.19
ZEB2NAT	-1.62	0.12	8.49	-0.12	0.22	73.00	2.42	1.86	0.00
ZFAS1	-1.12	0.18	19.72	0.68	0.53	46.39	2.48	2.96	0.00
Zfhx2as	2.52	1.24	0.00	0.11	0.28	63.34	-3.59	0.22	0.00

Table 4. **List of the analyzed lncRNAs**

	PAds / PaNs				PCas / PaNs				PCas / PAds			
Gene Name	**Score-d**	**FC**	**q-value**		**Score-d**	**FC**	**q-value**		**Score-d**	**FC**	**q-value**	
BC200	1.78	1.54	4.07		5.12	5.58	0.00	↑PCa	3.25	3.63	0.00	↑PCa
HAR1B	2.14	1.36	0.00		0.71	0.36	46.39		-2.16	0.26	0.00	↓PCa
HOXA3as	2.13	2.18	0.00	↑PAd	2.41	0.75	0.00		-0.91	0.34	15.12	
HOXA6as	2.61	3.51	0.00	↑PAd	5.83	3.00	0.00	↑PCa	0.25	0.85	29.30	
KCNQ1OT1	-2.23	0.12	0.00	↓PAd	-2.26	0.08	7.95		-1.15	0.67	15.12	
MEG3	-0.07	0.37	58.06		-1.44	0.14	29.45		-2.29	0.37	0.00	↓PCa
NEAT1	3.10	3.42	0.00	↑PAd	1.47	0.42	18.71		-3.25	0.12	0.00	↓PCa
SNHG6	-2.52	0.10	0.00	↓PAd	-3.26	0.08	0.00	↓PCa	-0.55	0.81	22.44	
WT1-as	-1.81	0.14	3.61	↓PAd	-0.08	0.32	73.00		1.73	2.31	1.75	↑PCa

Table 5. **SAM selected lncRNAs significantly altered in the indicated classes.** A significant q-value (< 5%) and the fold-change (FC) ≥ 2 and ≤ 0.5 (data not log2 transformed) were set as thresholds for significant differential expression.

4.3 LncRNAs validation analysis revealed a strong heterogeneity among human parathyroid tumors

The 9 significant lncRNAs were validated in a second independent cohort of parathyroid samples composed of 4 normal glands, 7 parathyroid carcinomas, 26 parathyroid adenomas and 6 atypical parathyroid adenomas (aPAds). By unsupervised analysis we identified three main samples clusters. Confirming previous data, PaNs and PCas were distinctly separated and PAds distributed in a variable way across all samples clusters, reflecting clinical and histological heterogeneity of the disease. Interestingly, aPAds were closer to PCas (Fig. 9A). Of note, samples in cluster 3 had a significative lncRNAs overexpression compared to cluster 1 and 2, as shown in box plots (Fig. 9B). Furthermore, samples in cluster 3 were characterized by a lower age of tumor onset (Fig. 9C).

A

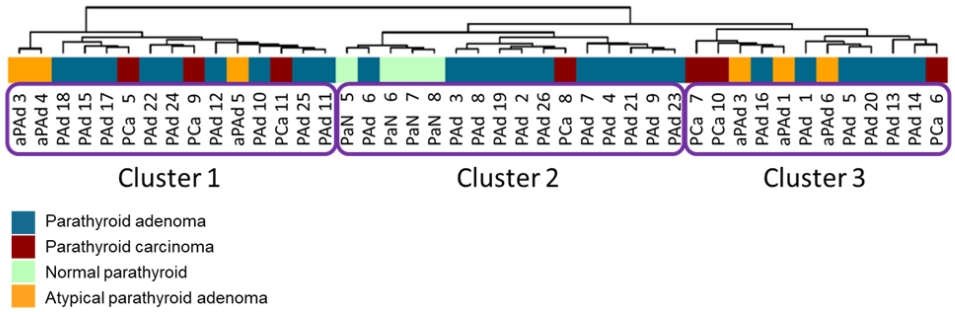
aPAd 3
aPAd 4
PAd 18
PAd 15
PAd 17
PCa 5
PAd 22
PAd 24
PCa 9
PAd 12
aPAd 5
PAd 10
PCa 11
PAd 25
PAd 11
PaN 5
PAd 6
PaN 6
PaN 7
PaN 8
PAd 3
PAd 8
PAd 19
PAd 2
PAd 26
PCa 8
PAd 7
PAd 4
PAd 21
PAd 9
PAd 23
PCa 7
PCa 10
aPAd 3
PAd 16
aPAd 1
PAd 1
aPAd 6
PAd 5
PAd 20
PAd 13
PAd 14
PCa 6
Cluster 1
Cluster 2
Cluster 3
Parathyroid adenoma
Parathyroid carcinoma
Normal parathyroid
Atypical parathyroid adenoma

B

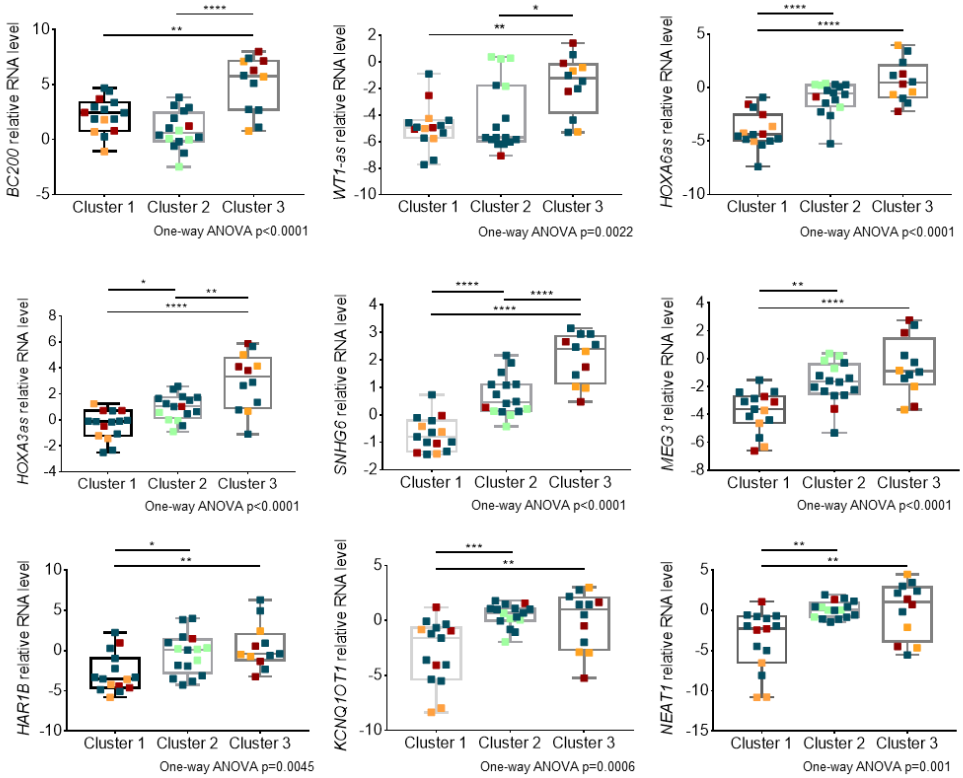
BC200 relative RNA level
Cluster 1 Cluster 2 Cluster 3
One-way ANOVA p<0.0001
WT1-as relative RNA level
One-way ANOVA p=0.0022
HOXA6as relative RNA level
One-way ANOVA p<0.0001
HOXA3as relative RNA level
One-way ANOVA p<0.0001
SNHG6 relative RNA level
One-way ANOVA p<0.0001
MEG3 relative RNA level
One-way ANOVA p<0.0001
HAR1B relative RNA level
One-way ANOVA p=0.0045
KCNQ1OT1 relative RNA level
One-way ANOVA p=0.0006
NEAT1 relative RNA level
One-way ANOVA p=0.001

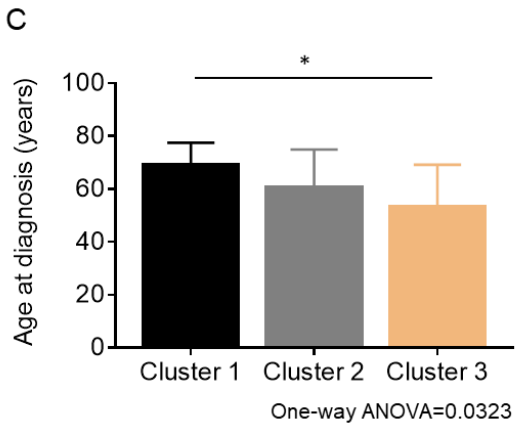

Figure 9. **LncRNAs validation analysis revealed a strong heterogeneity among human parathyroid tumors.** (A) Unsupervised Hierarchical Clustering dendrogram of 9 significative lncRNAs. (B) qRT-PCR analysis of 9 selected lncRNAs among the 3 clusters. Samples are normalized on 18S housekeeping gene. (C) Age at tumor diagnosis in the 3 clusters. All data are presented as mean ± SD. p-values are from parametric one-way ANOVA with Tukey post-test. *, P < 0.05; **, P < 0.01; ***, P < 0.001; ****, P < 0.0001.

4.4 Correlation of lncRNAs expression with genetic hallmark of parthyroid carcinomas

Parathyroid carcinomas are frequently characterized by inactivating mutations of the CDC73 tumor suppressor gene [107]. Notably, we observed that PCas 6, 7 and 10 from cluster 3 were mutated for CDC73 gene compared to PCas from cluster 1 and PCa 8 from cluster 2 (Table 6). Notably, these 3 carcinomas were characterized by an overexpression of BC200, HOXA3as, SNHG6 and WT1-as (Fig. 10A), suggesting their involvement in carcinomas aggressiveness. PCas from cluster 3 presented a growing trend in PTH, serum calcium and ionized calcium levels, compared to other 4 PCas (Fig. 10B).

Sample	Mutation	Mutation status
PCa 6	518_521 del4	*Germline*
PCa 7	415C>T	*Germline*
PCa 10	578_582 del5	*Somatic*

Table 6. **CDC73 mutations in patients with parathyroid carcinoma.**

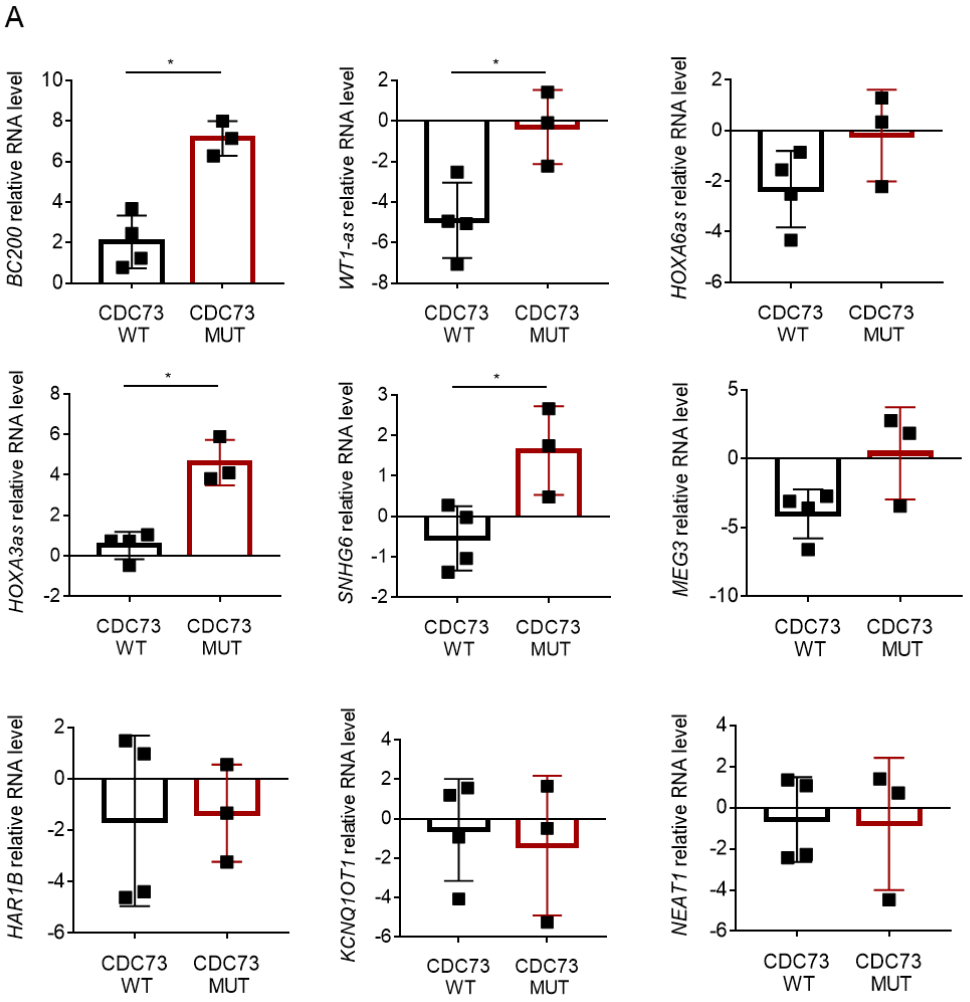

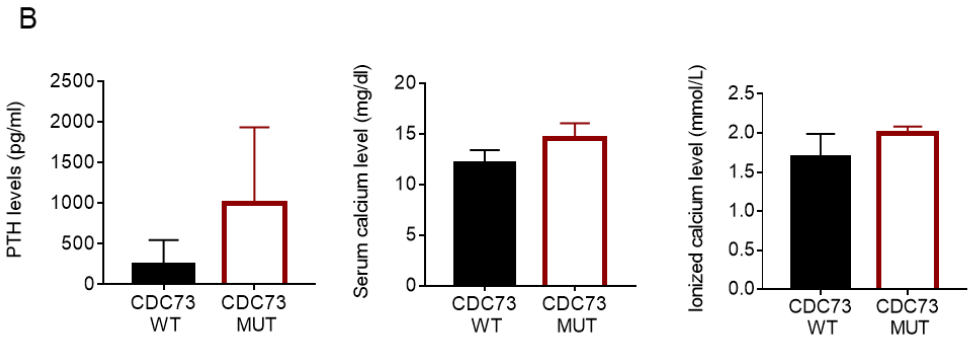

Figure 10. **LncRNAs upregulation characterized PCas with CDC73 mutations.** (A) qRT-PCR analysis of 9 significative lncRNAs evaluated in PCas mutated for CDC73 gene compared to WT PCas. (B) Analysis of PTH, serum calcium and ionized calcium levels in CDC73 mutated and WT PCas. All data were presented as mean ± SD. Samples are normalized on 18S housekeeping gene. P-values are from Mann-Whitney U-test. *, P ≤ 0.05.

Atypical adenomas of the parathyroid gland are a rare entity. These tumors are characterized by some features of PCas, but they lack evidence of invasive growth [108]. As previously showed in figure 3A, lncRNAs signature grouped aPAds in cluster 1 and cluster 3.

These data suggest that aPAds and PCas could be regulated by common mechanisms mediated by lncRNAs.

4.5 Identification of genetic alterations in parathyroid adenomas

Our results showed a considerable heterogeneity between PAds, scattered among three clusters. To better characterize PAds from a genomic point of view, we performed aCGH analysis on 24 PAds. Particularly, loss of heterozygosity (LOH) of short arm of chromosome 1 (Chr1-LOH) and LOH of long arm or the entire chromosome 11 (Chr11-LOH) were the two most frequent aberrations detected (8 and 10 PAds, respectively; fig. 11). No chromosomal alterations were detected in 7 of 24 adenomas. In table 7 all chromosome aberrations are indicated.

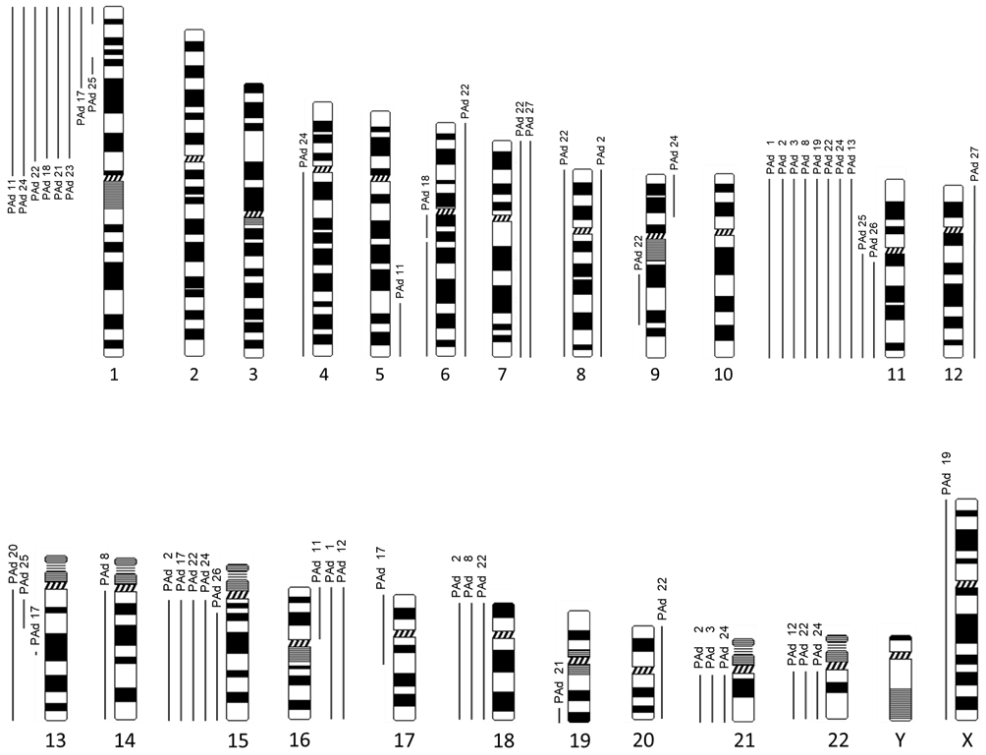

Figure 11. **Chromosome 11 LOH is the main frequent aberration among PAds**. Whole genome distribution of chromosomal alterations in PAds (n=17) as detected by aCGH (Agilent 8x60K microarray kit). Lines to the right of the chromosome indicate gain of chromosomal material. Lines to the left of the chromosome indicate loss of chromosomal material. No chromosomal alterations were detected in 7 of 24 PAds.

SAMPLE	Chr	Cytoband	Start	Stop	# probes	Gain	Loss	Aberration
PAd1	Chr11	p15.5 - p11.12	218,365	51,432,742	970	0	-0.700058	Monosomy (76.89%)
	Chr11	q11 - q25	55,110,047	134,868,407	1782	0	-0.708334	Monosomy (76.89%)
	Chr16	p13.3 - p11.1	154,314	35,045,499	762	0.526736	0	Trisomy
	Chr16	q11.2 - q24.3	46,564,557	90,111,263	1000	0.523115	0	Trisomy
PAd2	Chr 8	p23.3 - p11.21	293,177	42,821,662	768	0.411943	0	Trisomy
	Chr 8	q11.1 - q24.3	47,681,335	146,280,020	1635	0.418779	0	Trisomy
	Chr 11	p15.5 - p11.12	218,365	51,432,742	970	0	-0.484112	Monosomy (56.60%)
	Chr 11	q11 - q25	55,110,047	134,746,628	1781	0	-0.489132	Monosomy (56.60%)
	Chr 15	q11.1 - q26.3	20,102,541	102,383,473	1699	0	-0.541066	Monosomy (62.54%)
	Chr 18	p11.32 - p11.21	198,111	13,825,806	260	0	-0.600208	Monosomy (63.40%)
	Chr 18	q11.1 - q23	18,620,055	77,982,126	967	0	-0.499608	Monosomy (63.40%)
	Chr 21	q11.2 - q22.3	14,640,392	48,067,924	723	0	-0.538779	Monosomy (62.45%)
PAd3	Chr 11	p15.5 - p11.12	218,365	51,432,742	970	0	-0.561385	Monosomy (64.34%)
	Chr 11	q11 - q25	55,110,047	134,746,628	1781	0	-0.569484	Monosomy (64.34%)
	Chr 21	q11.2 - q22.3	15,372,467	48,056,450	715	0	-0.591331	Monosomy (67.22%)
PAd8	Chr 11	p15.5 - p11.12	218,365	51,432,742	970	0	-0.639985	Monosomy (71.66%)
	Chr 11	q11 - q25	55,110,047	134,868,407	1781	0	-0.644643	Monosomy (71.66%)
	Chr 14	q11.2 - q32.33	20,253,739	107,258,824	1730	0.25343	0	Trisomy (38.34%)
	Chr 18	p11.32 - p11.21	142,096	14,748,636	273	0	-0.639547	Monosomy (70.76%)
	Chr 18	q11.1 - q23	18,539,853	77,982,126	968	0	-0.62522	Monosomy (70.76%)
PAd11	Chr 1	p36.33 - p11.2	852,863	121,184,327	2473	0	-0.764997	Monosomy (81.31%)
	Chr 5	q31.1 - q35.3	133,624,982	180,684,501	962	0.23779	0	Trisomy (35.87%)
	Chr 16	p13.3 - p11.2	154,314	33,604,468	749	0.502353	0	Trisomy
PAd12	Chr 16	p13.3 - p11.1	154,314	34,989,883	761	0.604304	0	Trisomy
	Chr 16	q11.2 - q24.3	46,564,557	90,111,263	1000	0.56603	0	Trisomy
	Chr 22	q11.1 - q13.33	17,096,855	51,178,264	899	0	-0.711159	Monosomy (77.74%)
PAd13	Chr 7	p22.3 - p11.2	92,532	57,494,441	993	0.386698	0	Trisomy (56%)
	Chr 7	q11.21 - q36.3	62,516,153	159,088,636	2054	0.331808	0	Trisomy (56%)
	Chr 11	p15.5 - p11.12	218,365	51,432,742	970	0	-0.543991	Monosomy (63%)
	Chr 11	q11 - q25	55,110,047	134,746,628	1780	0	-0.558902	Monosomy (63%)
PAd17	Chr 1	p36.33 - p31.3	759,762	68,732,755	1542	0	-0.745107	Monosomy (81.08%)
	Chr 13	q21.33	69,666,001	71,618,625	25	0	-0.787228	Monosomy (84.33%)
	Chr 15	q11.1 - q26.3	20,102,541	102,383,473	1700	0	-0.760437	Monosomy (81.90%)
	Chr 17	p13.2 - p11.2	4,027,661	22,078,577	476	0	-0.72628	Monosomy (79.42%)
	Chr 17	q11.1 - q21.2	25,403,446	40,490,841	463	0	-0.745786	Monosomy (79.42%)
PAd18	Chr 1	p36.33 - p13.3	759,762	109,922,384	2219	0	-0.249637	Monosomy (31.82%)
	Chr 6	q11.1 - q14.1	62,854,306	76,412,473	208	0	-0.320288	Monosomy (39.79%)
	Chr 6	q15 - q27	92,045,694	169,426,640	1301	0	-0.219128	Monosomy (28.17%)

PAd19	Chr 11	p15.5 - p11.12	218,365	51,432,742	970	0	-0.74332	Monosomy (80.25%)
	Chr 11	q11 - q25	55,110,047	134,868,407	1781	0	-0.75237	Monosomy (80.25%)
	Chr 12	p13.33 - p11.1	289,648	34,345,585	731	0.439969	0	Trisomy (71.32%)
	Chr 12	q12 - q24.33	38,572,677	133,819,092	1970	0.457154	0	Trisomy (71.32%)
	Chr X	p22.33 - p11.21	61,091	58,051,765	1084	0	-0.686178	Monosomy (76.03)
	Chr X	q11.1 - q28	61,931,689	155,190,083	1596	0	-0.707851	Monosomy (76.03)
PAd20	Chr 13	q11 - q34	19,296,544	115,059,020	1716	0	-0.534137	Monosomy (67.87)
PAd21	Chr 1	p36.33 - p13.3	759,762	109,445,834	2202	0	-0.650618	Monosomy (72.76%)
	Chr 19	q13.31 - q13.43	43,810,421	59,092,570	671	0	-0.610701	Monosomy (69.05%)
PAd22	Chr 1	p36.33 - p13.2	759,762	115,489,021	2365	0	-0.212972	Monosomy (24.45%)
	Chr 6	p25.3 - p11.2	170,426	58,398,792	1261	0.310116	0	Trisomy (44.53%)
	Chr 6	q11.1 - q27	61,982,931	170,890,108	1788	0.269219	0	Trisomy (44.53%)
	Chr 7	p22.3 - p11.2	92,532	57,323,498	1011	0.280434	0	Trisomy (42.84%)
	Chr 7	q11.21 - q36.3	63,449,575	159,088,636	2049	0.284972	0	Trisomy (42.84%)
	Chr 8	p23.3 - p11.1	524,066	43,333,638	778	0	-0.19901	Monosomy (28.05%)
	Chr 8	q11.1 - q24.3	47,868,796	146,280,020	1634	0	-0.237824	Monosomy (28.05%)
	Chr 9	q21.11 - q32	71,151,735	116,113,138	794	0	-0.20703	Monosomy (26.73%)
	Chr 11	p15.5 - p11.12	218,365	51,432,742	970	0	-0.669877	Monosomy (74.73%)
	Chr 11	q11 - q25	55,110,047	134,746,628	1781	0	-0.683793	Monosomy (74.73%)
	Chr 15	q11.2 - q26.3	22,925,956	102,369,897	1680	0	-0.232404	Monosomy (29.71%)
	Chr 18	p11.32 - p11.21	861,334	13,731,571	246	0	-0.235176	Monosomy (29.59%)
	Chr 18	q11.1 - q23	18,650,189	77,982,126	966	0	-0.227406	Monosomy (29.59%)
	Chr 20	p13 - p11.1	170,826	26,075,841	485	0.324333	0	Trisomy (46.23%)
	Chr 20	q11.21 - q13.33	29,972,876	62,664,464	742	0.286587	0	Trisomy (46.23%)
	Chr 22	q11.1 - q13.33	17,096,855	51,043,490	893	0	-0.251751	Monosomy (32.05%)
PAd23	Chr 1	p36.33 - p13.3	759,762	110,299,358	2232	0	-0.284609	Monosomy (35.85%)
PAd24	Chr 1	p36.33 - p11.2	759,762	121,281,170	2475	0	-0.674207	Monosomy (74.45%)
	Chr 4	q11 - q35.2	52,689,101	190,713,650	2239	0	-0.693439	Monosomy (76.29%)
	Chr 9	p24.3 - p13.1	271,257	38,663,271	655	0.448194	0	Trisomy (72.83%)
	Chr 11	p15.5 - p11.12	218,365	51,432,742	970	0	-0.68225	Monosomy (75.60%)
	Chr 11	q11 - q25	55,110,047	134,746,628	1781	0	-0.688566	Monosomy (75.60%)
	Chr 15	q11.1 - q26.3	20,102,541	102,383,473	1699	0	-0.677854	Monosomy (74.99%)
	Chr 21	q11.2 - q22.3	14,640,392	48,067,924	723	0	-0.690215	Monosomy (76.03%)
	Chr 22	q11.1 - q13.33	17,096,855	51,177,360	898	0	-0.636326	Monosomy (71.30%)
PAd25	Chr 1	p36.33 - p36.23	759,762	8,343,813	117	0	-0.27625	Monosomy (34.82%)
	Chr 1	p34.1 - p32.3	44,683,334	54,869,282	255	0	-0.3011	Monosomy (37.66%)
	Chr 11	q11 - q25	55,375,127	130,864,000	1704	0	-0.276914	Monosomy (34.94%)
	Chr 13	q12.11 - q14.3	21,907,775	51,989,186	647	0	-0.675003	Monosomy (74.73%)
PAd26	Chr 11	q12.1 - q25	59,739,027	134,868,407	1682	0	-0.78755	Monosomy (84.17%)
	Chr 15	q13.1 - q26.3	29,641,152	102,383,473	1573	0	-0.788796	Monosomy (84.25%)

Table 7. **Chromosome aberrations in PAds analyzed for aCGH.** Chr1-LOH (blue) and Chr11-LOH (purple) are the two most frequent aberrations detected.

4.6 LncRNAs profiling and the genetic background in parathyroid adenomas

The loss of heterozygosity of chromosome 11 in parathyroid adenomas is already known in literature [109]. To identify a possible correlation between the 2 most frequent chromosome aberrations previously identified and 9 selected lncRNAs, we evaluated lncRNAs levels in 24 PAds. Results showed that PAds with Chr1-LOH had modulation in SNHG6 levels (p=0.0246) whereas HAR1B was strongly upregulated in Chr11-LOH PAds ((p<0.0001; Fig. 12). These data support the idea of a possible involvement of the 2 chromosomes in SNHG6 and HAR1B regulation in parathyroid adenomas.

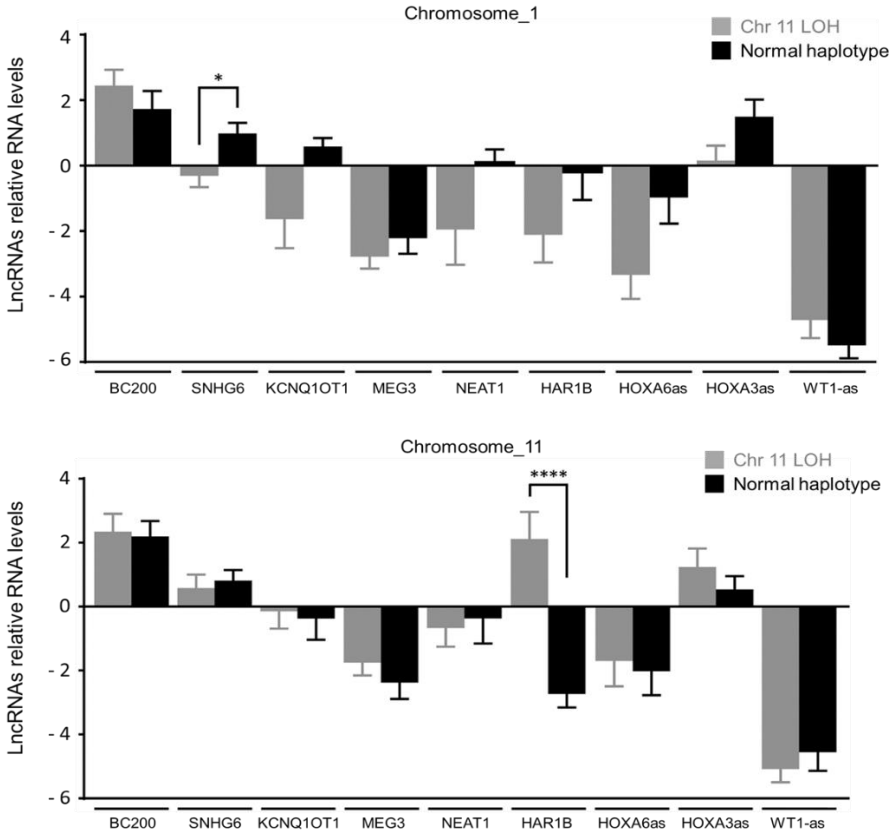

Figure 12. **LncRNAs modulation in PAds with chromosome 1 and 11 LOH.** Nine selected lncRNAs expression was evaluated in 24 PAds through quantitative RT-PCR. For each tested gene, the expression level is presented as mean ± SEM. P-values were from Mann-Whitney U-test. *, P < 0.05, **** < 0.0001.

4.7 Chromosome 11 LOH correlates with HAR1B upregulation

As reported in figure 11 and consistently with previously published literature [110], chromosome 11 alteration is one of the most crucial events in the onset of parathyroid adenomas. We report here that PAds with Chr11-LOH (1X PAds) are characterized by a significative upregulation of HAR1B lncRNA compared to PAds with normal haplotype (2X PAds; fig. 13A). Then, we hypothesized that there could be one or more key elements on Chr11 capable to inhibit HAR1B expression in 2X PAds and whose loss induces HAR1B overexpression. In Gene Cards® HUMAN GENE DATABASE, HAR1B promoter is the target of some transcription factors including EZH2, EED and SUZ12 (Fig. 13B), parts of the Polycomb repressive complex 2 (PRC2). EZH2 is the catalytic subunit of the PRC2 complex that, through EED binding, promotes trimethylation of histone H3 lysine 27 (H3K27me3; [111]. Notably, EED subunit of PRC2 maps on chromosome 11 at locus 11q14.2. Therefore, we supposed that in absence of EED (1X PAds), the PRC2 complex is inactive, thus unable to repress HAR1B transcription (Fig. 13C). To provide evidence in this direction we first evaluated expression levels of EZH2 target genes: *AXIN2*, *CCND1*, *CDH1* and *CDKN1A* (Fig. 13D), in PAds with or without Chr11-LOH. With the exception for CDH1, EZH2 target genes were significantly modulated between 1X and 2X PAds.

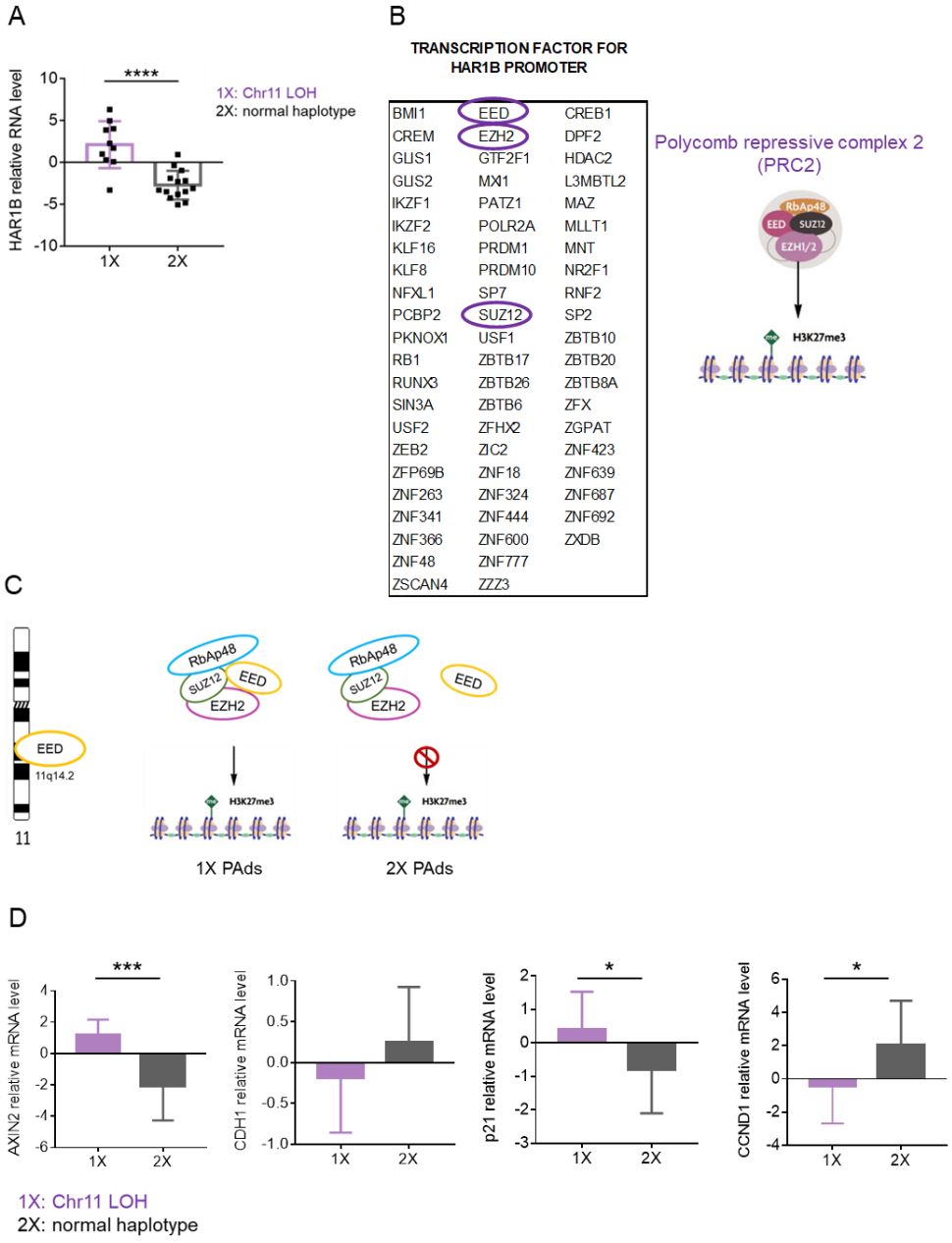

Figure 13. **HAR1B is upregulated in PAds with chromosome 11 LOH**. (A) qRT-PCR of HAR1B levels in PAds with (1X) or without (2X) Chr11-LOH. (B) List of transcription factor that could regulate HAR1B transcription. Data were from Gene Cards® HUMAN GENE DATABASE. EED, EZH2 and SUZ12 (purple circle) belong to Polycomb Repressive Complex 2 (PRC2). (C) Proposed model for HAR1B regulation. (D) qRT-PCR analysis of EZH2 target genes in PAds with Chr11 LOH

compared to PAds with a normal haplotype. All data are presented as mean ± SD. P-values were from Mann-Whitney U-test. *, P < 0.05; **, P < 0.01; ***, P < 0.001; ****, P < 0.0001.

EZH2 and *EED* levels were also evaluated at protein level by WB analysis. Despite EZH2 and EED mRNA levels did not differ between 1X and 2X PAds (Fig.14A), both proteins were more expressed in 2X PAds (Fig. 14B).

PRC2 methylates, through the catalytic subunit EZH2, the lysine 27 in histone H3, a modification associated with epigenetic gene silencing [112]. Since our hypothesis was that PRC2 complex could be involved in HAR1B regulation we looked at H3K27me3 protein levels. Preliminary WB blot analysis showed that H3K27me3 is more expressed in 2X PAd compared to 1X PAd (Fig.14B), strengthen the hypothesis of a different PRC2 complex activation between 1X and 2X PAds.

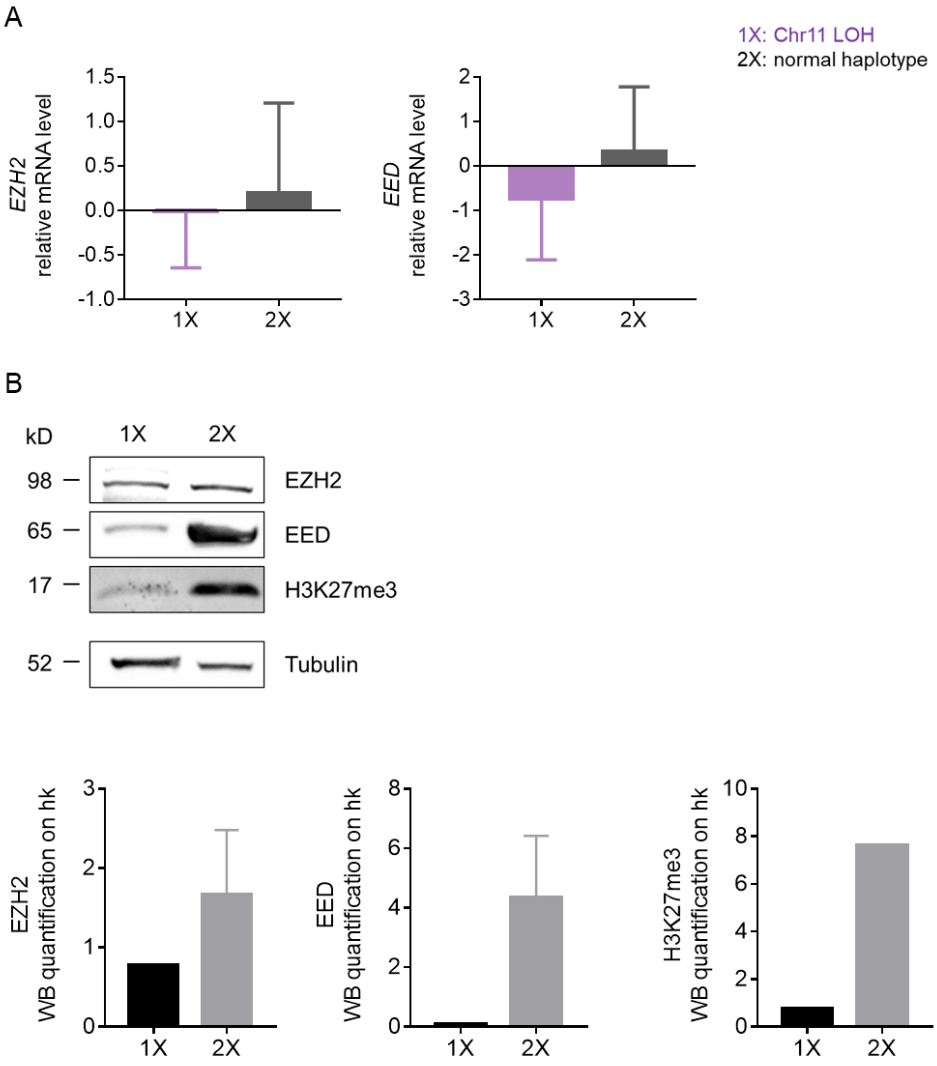

Figure 14. **PCR2 complex is activated in PAds without chromosome 11 LOH**. (A) qRT-PCR analysis of EZH2 and EED in PAds with or without Chr11-LOH. Data are presented as mean ± SD. P-values were from Mann-Whitney U-test. (B) Western blot analysis of EZH2, EED and H3K27me3 in 1X PAds (n=1) compared to 2X PAds (n=2). For H3K27me3 WB analysis, only one 2X PAd protein extract was available. Tubulin is shown as the loading control. The graphs represent the WB quantification.

4.8 Focus on HAR1B regulation

Based on these results, we hypothesized that HAR1B promoter could be subjected to epigenetic silencing (i.e. methylation) in 2X PAds, thus explaining its downregulation. To test this hypothesis, we treated HEK293 cells with the demethylating agent 5-azacytidine (5-AZA) at different concentration and we analyzed HAR1B mRNA levels (Fig. 15A). After 48 hours, 5-AZA was able to restore HAR1B levels. Finally, to test whether HAR1B downregulation was mediated by EZH2, HEK293 cells were treated with Tazemetostat (EPZ-6438; TAZ), a selective inhibitor of EZH2 enzymatic activity. After 48 hours, 1 µM TAZ treatment induced an overexpression of HAR1B mRNA (Fig. 15B), suggesting that EZH2 could be directly involved in HAR1B methylation. These functional assays are ongoing in primary parathyroid adenomas cultures together with quantitative methylation specific PCR analysis (qMSP), to detect hypermethylation of HAR1B promoter.

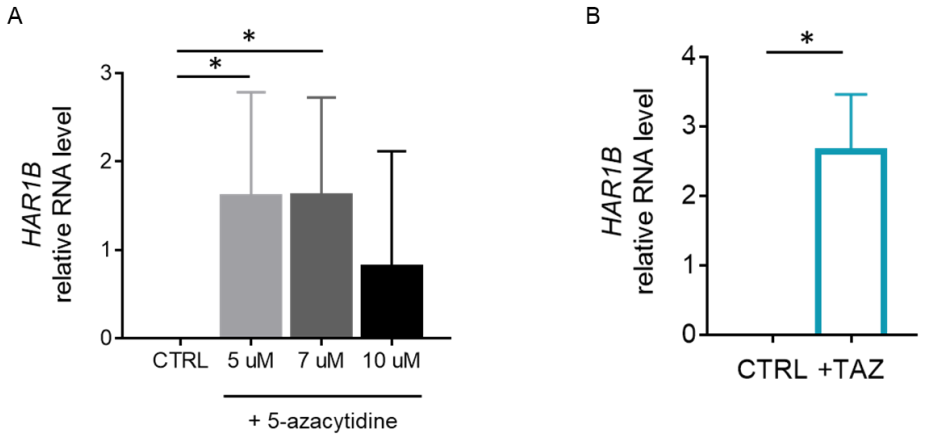

Figure 15. **EZH2 inhibition restored HAR1B levels, in HEK293 cells**. (A) qRT-PCR analysis of HAR1B after 5-azacytidine and (B) Tazemetostat (1µM) treatment, for 48h. Data are presented as mean ± SD of three independent experiments. P-values were from Mann-Whitney U-test. *, $P < 0.05$.

4.9 HAR1B involvement in Wnt/beta-catenin pathway

HAR1B is expressed in human adult brain, testis and ovary [113]. Moreover, it is repressed by REST in Huntington disease [114] but its functional role is still unknown. To elucidate the molecular pathways in which HAR1B is involved, we silenced HAR1B in HEK293 cells (Fig. 16A) and we analyzed the expression of genes involved in carcinogenesis using the “Human Molecular Mechanisms of Cancer”- array plate (Fig. 16B). Preliminary data showed that the 2 most upregulated genes in cells silenced for HAR1B were LEF1 and WNT1 (Fig. 16C), two components of the canonical Wnt/beta-catenin pathway. Although this pathway was characterized in parathyroid carcinomas, its involvement in parathyroid adenomas was not well understood [31]. For these reasons, next step will be to evaluate the involvement of Wnt pathway in primary parathyroid adenomas, *in vitro*, and its relation with HAR1B.

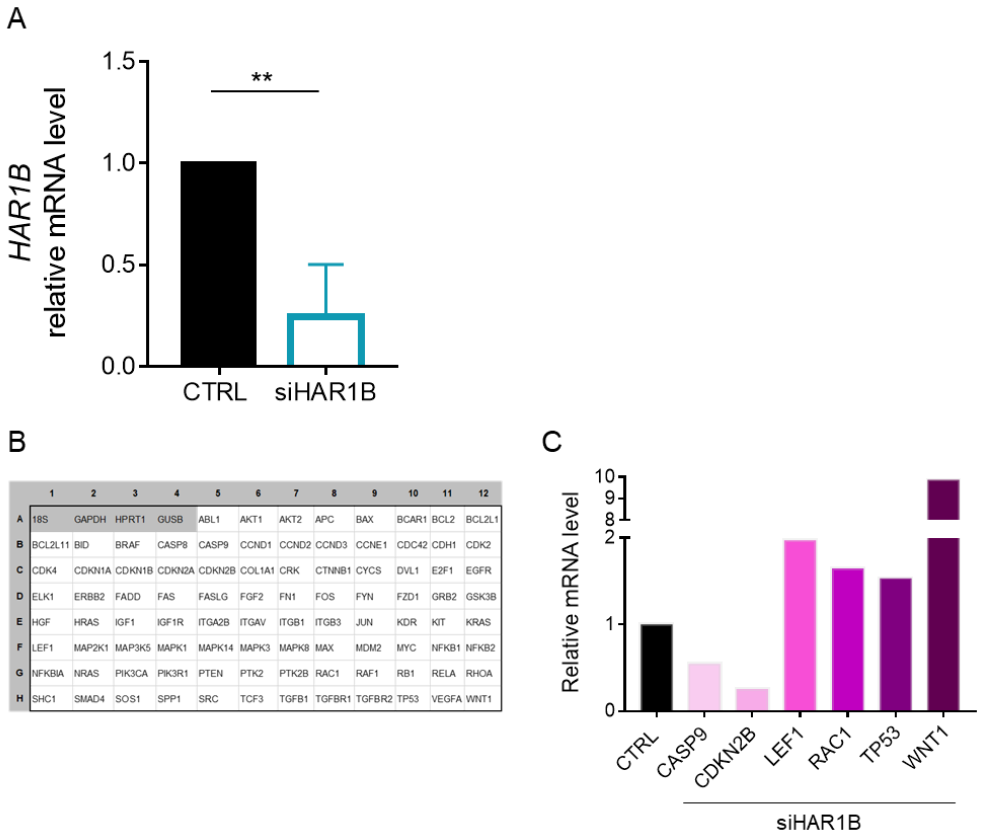

	1	2	3	4	5	6	7	8	9	10	11	12
A	18S	GAPDH	HPRT1	GUSB	ABL1	AKT1	AKT2	APC	BAX	BCAR1	BCL2	BCL2L1
B	BCL2L11	BID	BRAF	CASP8	CASP9	CCND1	CCND2	CCND3	CCNE1	CDC42	CDH1	CDK2
C	CDK4	CDKN1A	CDKN1B	CDKN2A	CDKN2B	COL1A1	CRK	CTNNB1	CYCS	DVL1	E2F1	EGFR
D	ELK1	ERBB2	FADD	FAS	FASLG	FGF2	FN1	FOS	FYN	FZD1	GRB2	GSK3B
E	HGF	HRAS	IGF1	IGF1R	ITGA2B	ITGAV	ITGB1	ITGB3	JUN	KDR	KIT	KRAS
F	LEF1	MAP2K1	MAP3K5	MAPK1	MAPK14	MAPK3	MAPK8	MAX	MDM2	MYC	NFKB1	NFKB2
G	NFKBIA	NRAS	PIK3CA	PIK3R1	PTEN	PTK2	PTK2B	RAC1	RAF1	RB1	RELA	RHOA
H	SHC1	SMAD4	SOS1	SPP1	SRC	TCF3	TGFB1	TGFBR1	TGFBR2	TP53	VEGFA	WNT1

Figure 16. **HEK293 cells silenced for HAR1B expression show a modulation of Wnt pathway related genes.** (A) qRT-PCR analysis of HAR1B in HEK293 cells (48h). B2M was used as loading control. Data are presented as mean ± SD of three independent experiments. P-value was from Mann-Whitney U-test. (B) Representation of the TaqMan® - Human Molecular Mechanisms of Cancer – 96-Well FAST plate. (C) mRNA levels of the main modulated genes in siHAR1B cells compared to cells transfected with CTRL siRNA. Data are normalized on the mean of the 4 housekeeping genes.

4.10 MEN1 silencing induces HAR1B upregulation in primary parathyroid adenomas cultures

Our data showed that PAds with Chr11-LOH (nr=10) were characterized by a significative downregulation of MEN1 transcription levels, compared to PAds without LOH (nr=14; fig. 17A). MEN1 is a protein that acts as an onco-suppressor in endocrine tissues. Notably, MEN1 maps on chromosome 11 [115]. Xu et al. [116], demonstrated that MEN1 can repress its target genes increasing H3K27 trimethylation. Due to these evidences and our previous data, in which HAR1B transcription levels were regulated by EZH2 (paragraph 4.8), we investigated if MEN1 could influence HAR1B expression. To this aim we kept in culture 4 parathyroid adenomas and we silenced them for MEN1 expression. From a small portion of each samples, we previously extracted the DNA and we performed aCGH analysis, to profile them for chromosome 11 aberration. Two PAds, PAd27 and PAd29, were characterized by Chr11-LOH, compared to PAd28 and PAd30 (Fig. 17B). After MEN1 silencing, PAds with normal haplotype showed an increase in HAR1B levels (Fig. 17C). These findings suggest that MEN1 could regulate, directly or indirectly, HAR1B expression. Moreover, since we previously demonstrated that HAR1B levels increased after EZH2 inhibition, we supposed a possible cooperation between MEN1 and PRC2 complex.

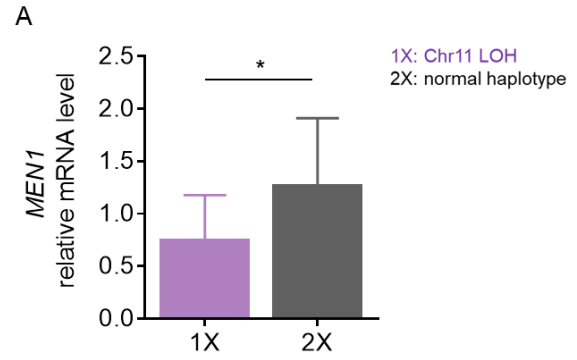

B

PAd27	Chr 11	p15.5 - p1	218,365	51,432,742	970	0	-0.57783	Monosomy (66%)
	Chr 11	q11 - q25	55,110,047	134,746,628	1781	0	-0.59431	Monosomy (66%)
PAd29	Chr 11	p15.5 - p1	218,365	51,432,742	970	0	-0.52755	Monosomy (61%)
	Chr 11	q11 - q25	55,110,047	134,746,628	1781	0	-0.53617	Monosomy (61%)

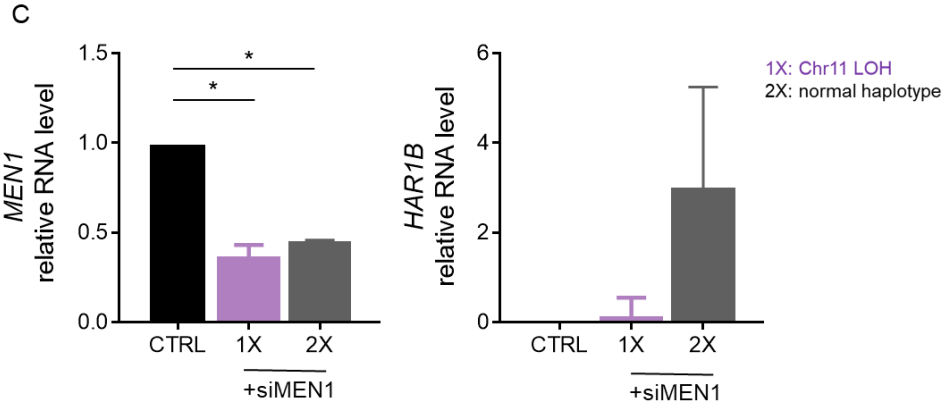

Figure 17. **MEN1 silencing induces HAR1B upregulation in parathyroid adenomas**. (A) qRT-PCR analysis of MEN1 levels in 24 PAds with or without Chr11-LOH. Data are presented as mean ± SD. P-values were from Mann-Whitney U-test. (B) aCGH analysis of 4 PAds. Two PAds did not show chromosomal alterations. Lines to the left of the chromosome indicate loss of chromosomal material. (C) qRT-PCR analysis of MEN1 and HAR1B in 4 PAds (2 1XPAds and 2 2XPAds). Data are presented as mean ± SD. For each PAd, the untreated cells were used as control.

4.11 PTH, serum calcium and ionized calcium levels are not influenced by HAR1B lncRNA

Parathyroid glands are responsible for PTH secretion when serum calcium levels are low. This condition stimulates calcium release from bone and the synthesis of active vitamin D [117]. On the contrary, in parathyroid tumors there is both an overproduction of PTH hormone and calcium increment in the blood (hypercalcemia; [118]). Here, we analyzed PTH, serum and ionized calcium levels in PAds with or without Chr11-LOH, to evaluate if there is a correlation with HAR1B expression. Notably, there were no differences in PTH, serum and ionized calcium levels in adenomas with Chr11-LOH compared to other samples (Fig. 18). These data suggest not only that HAR1B is not related to the secretory function of parathyroid glands but also that biochemical parameters in parathyroid adenomas are not affected by loss of heterozygosity of chromosome 11.

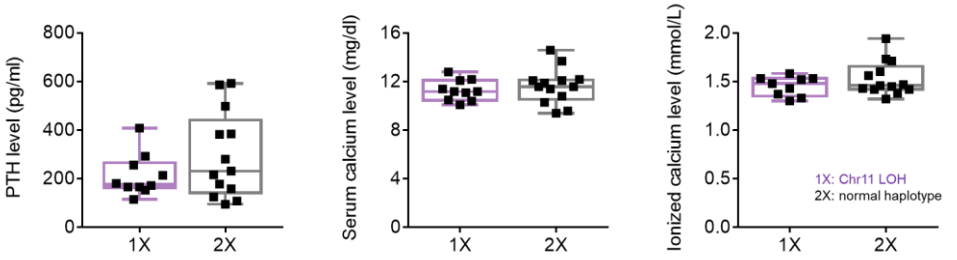

Figure 18. **PTH, serum calcium and ionized calcium levels in parathyroid adenomas**. 1X: PAds with Chr-11 LOH; 2X: PAds with normal haplotype.

5. DISCUSSION

Parathyroid glands are part of the human endocrine system responsible for parathormone (PTH) production which helps to maintain an appropriate calcium level in the blood [119]. In response to low calcium levels, PTH secretion induces calcium release from the bone through osteoclasts stimulation and osteoblasts inhibition [4]. Additionally, PTH induces calcium and magnesium reabsorption and stimulates the production of vitamin D in the kidneys. PTH release is regulated by a negative feedback loop achieved by blood calcium levels. Abnormal hyperactivation of parathyroid glands results in hyperparathyroidism, a disorder characterized by inappropriate PTH overproduction with a consequent hypercalcemia. This condition may derive either from adenoma (80-85%), hyperplasia (10-15%) or malignant neoplasm (<1%) of the parathyroid gland and for this reason it is difficult to diagnose these tumors before surgery [120]. Hence, the importance to identify new potential diagnostic biomarkers able to distinguish among parathyroid histotypes. Recently, it has been demonstrated that epigenetic aberrations are implicated in endocrine tumors [121], [122]. Although long non-coding RNAs are a class of RNAs with no protein coding function, they are key regulators of both physiological processes and cancer development [68], [96], [123]. To date, there are no study about long non-coding signatures in parathyroid tumors.

In this study, we described that normal parathyroid glands (PaNs), adenomas (PAds) and carcinomas (PCas), were characterized by specific lncRNAs signatures, which were able to distinguish among the three tissue types. This data is consistent with the previously published tissue-specificity of lncRNAs [124]. Specifically, KCNQ1OT1 and SNHG6 were enriched in PaNs, HAR1B, HOXA3as, MEG3 and NEAT1 expression characterized PAds, whereas BC200 and HOXA6as were significantly upregulated in PCas

compared to PaNs. As previously seen with the microRNAs [105], an elevated variability in lncRNAs expression among samples of the same histotype was observed. Specifically, the unsupervised analysis identified 3 main clusters among parathyroid samples in which normal glands showed a different lncRNAs expression profile compared to carcinomas. Atypical adenomas showed a lncRNAs pattern more similar to carcinomas. Parathyroid adenomas had a heterogeneous distribution and arranged in all 3 samples' groups. Interestingly, unsupervised analysis revealed that samples in cluster 3 were characterized by a general lncRNAs upregulation and by a lower age of tumor onset, compared to samples with lncRNAs downregulation. In line with previously published report [125], BC200 was the most upregulated lncRNA in carcinomas compared to normal glands.

Parathyroid carcinomas are generally associated with CDC73 gene mutations [126]. CDC73 gene codifies for the tumor suppressor protein parafibromin. In physiological conditions, parafibromin inhibits *CYCLIN D1* and *c-MYC* genes through SUV39H1 histone methyltransferase recruitment. In pathological conditions, CDC37 binds β-catenin and activates Wnt pathway [28], [127]. We report here that CDC73-mutated carcinomas, all grouped in cluster 3, were characterized by a general lncRNAs upregulation compared to other 4 PCas. Parathyroid carcinomas are characterized by PTH and calcium hypersecretion [21]. Our data revealed that CDC73-mutated samples showed a trend in increased PTH, serum calcium and ionized calcium levels. Atypical parathyroid adenomas are rare entities that share some histologic features with carcinomas but do not present capsule or vascular invasion [128]. Our results suggested that, at the molecular level, atypical adenomas may be more similar to carcinomas, at least concerning lncRNAs expression pattern.

The unsupervised analysis showed that parathyroid adenomas were distributed across the 3 clusters, confirming the heterogeneous nature of these tumors [129]. Chromosome 11 loss of heterozygosity (Chr11-LOH) is

a well described genomic abnormality in parathyroid adenomas. In particular, this deletion was shown to be the key event in adenomas onset [130], [131]. In agreement with these data, aCGH analysis showed that Chr11-LOH was the most frequent aberration among parathyroid adenomas (10 out of 24 PAds), followed by Chr1-LOH (8 out of 24 PAds). In the present work we showed that in adenomas characterized by Chr11-LOH (1X-PAds), HAR1B was significantly upregulated compared to samples with a normal haplotype (2X-PAds). We hypothesized that this might be to the presence of a factor on chromosome 11 that physiologically inhibits HAR1B levels. In Gene Cards® HUMAN GENE DATABASE, HAR1B promoter is target of EZH2, EED and SUZ12, components of Polycomb Repressive Complex 2 (PRC2). PRC2 mediates gene silencing through its catalytic subunit EZH2 that, together with EED, trimethylates lysine 27 on histone H3 (H3K27me3; [52] [132]–[134]). Finally, EED maps on chromosome 11 locus 11q14.2 [135]. Here, we reported that *AXIN2* and *CDKN1A*, two EZH2 target genes, were downregulated in 2X-PAds. We also found that H3K27me3 levels were higher in 2X-PAds compared to PAds with Chr11-LOH. These data support the concept that in partial absence of chromosome 11, and consequently of EED, the PRC2 complex is less active. Moreover, we showed that EZH2 selective inhibition with Tazemetostat restored HAR1B levels in HEK293 cells.

MEN1 gene maps on chromosome 11 (locus 11q13.1) and codifies for the Multiple Endocrine Neoplasia 1, a tumor suppressor protein mutated in 30% of sporadic parathyroid adenomas [6]. Interestingly, we found that HAR1B levels increased after MEN1 silencing, in primary parathyroid adenomas with normal haplotype.

It has been demonstrated that HAR1B is expressed in adult brain, testis and ovary but its functional role in normal and pathological tissues remains unknown [113]. Here, we showed that HAR1B silencing in HEK293 cells induced an upregulation of LEF1 and WNT1, two components of the

canonical Wnt/β-catenin pathway [136], and an upregulation of RAC1, an activator of the same pathway [137]. Conversely, CASP9 and CDKN2B were the two most downregulated genes in HEK293 cells silenced for HAR1B expression.

Finally, we also analyzed whether circulating calcium levels were correlated with HAR1B expression in PAds. Our data showed that there was no difference in PTH, serum and ionized calcium levels comparing parathyroid adenomas with or without Chr11-LOH, suggesting that HAR1B is not related to the secretory function of parathyroid glands.

Further studies are needed to better characterize at the genome and epigenomic level parathyroid tumors and to better elucidate lncRNAs roles in these diseases. Moreover, other experiments are necessary to better investigate the role of HAR1B in parathyroid adenomas pathobiology.

6. CONCLUSIONS

Parathyroid tumors are rare endocrine diseases whose diagnosis is complicated due to their elevated cellular and molecular heterogeneity. Moreover, there are no specific histological and molecular features that help to distinguish preoperatively parathyroid adenomas, carcinomas and atypical adenomas.

LncRNAs are important players in tumor progression. To date, there is no description of lncRNAs profile in human parathyroid tumors. To this aim, we profiled parathyroid tissues for lncRNAs expression for the identification of novel diagnostic biomarkers.

Our findings show that human parathyroid tumors are characterized by different lncRNAs signatures, confirming the elevated heterogeneity of this disease. In particular, our study identifies BC200 as an interesting candidate biomarker for the diagnosis of parathyroid carcinomas. Further, we show that CDC73-mutated carcinomas overexpress the majority of lncRNAs. To confirm our findings, we will increase the number of carcinoma samples and we will analyze the correlation between lncRNAs expression and CDC73 mutation status.

Finally, our results shed light on a new lncRNA, HAR1B, suggesting a novel player in parathyroid adenomas pathobiology. It is possible that the epigenetic regulation of HAR1B is mediated by PRC2-mediated methylation process with MEN1 cooperation. It will be interesting to determine the role of HAR1B in parathyroid adenomas and to study the molecular mechanisms in which HAR1B is involved.

7. BIBLIOGRAPHY

[1] D. Carlson, “Parathyroid pathology hyperparathyroidism and parathyroid tumors,” *Arch. Pathol. Lab. Med.*, 2010.

[2] S. Gad, M. Elsamie, and Y. Saleh, “Parathyroid gland injuries during total and subtotal thyroidectomy,” *Menoufia Med. J.*, vol. 28, no. 4, p. 807, 2015.

[3] K. D. Schlüter, C. Katzer, and H. M. Piper, “A N-terminal PTHrP peptide fragment void of a PTH/PTHrP-receptor binding domain activates cardiac ETAreceptors,” *Br. J. Pharmacol.*, vol. 132, no. 2, pp. 427–432, 2001.

[4] P. H. Carter and E. Schipani, “The roles of parathyroid hormone and calcitonin in bone remodeling: prospects for novel therapeutics.,” *Endocr. Metab. Immune Disord. Drug Targets*, vol. 6, no. 1, pp. 59–76, 2006.

[5] M. Oliwia Anna Segiet and P. Mariusz Deska, MD, Marek Michalski, PhD, Jacek Gawrychowski, MD, PhD, Romuald Wojnicz, MD, “Molecular profiling in primary hyperparathyroidism Oliwia,” *Wiley Period. Inc. Head Neck*, vol. 37, pp. 299–307, 2014.

[6] F. Farnebo *et al.*, “Alterations of the MEN1 gene in sporadic parathyroid tumors,” *J. Clin. Endocrinol. Metab.*, vol. 83, no. 8, pp. 2627–2630, 1998.

[7] V. Busygina and A. E. Bale, “Multiple endocrine neoplasia type 1 (MEN1) as a cancer predisposition syndrome: Clues into the mechanisms of MEN1-related carcinogenesis,” *Yale J. Biol. Med.*, vol. 79, no. 3–4, pp. 105–114, 2006.

[8] C. J. Lips, K. M. Dreijerink, and J. W. Hoppener, “Variable clinical expression in patients with a germline MEN1 disease gene mutation: clues to a genotype-phenotype correlation,” *Clinics (Sao Paulo).*, vol. 67 Suppl 1, no. 7, pp. 49–56, 2012.

[9] S. K. Agarwal *et al.*, “Menin interacts with the AP1 transcription factor JunD and represses JunD-activated transcription,” *Cell*, vol. 96, no. 1, pp. 143–152, 1999.

[10] T. A. Milne *et al.*, “Menin and MLL cooperatively regulate expression of cyclin-dependent kinase inhibitors.,” *Proc. Natl. Acad. Sci. U. S. A.*, vol. 102, no. 3, pp. 749–54, 2005.

[11] K. M. A. Dreijerink, K. W. Mulder, G. S. Winkler, J. W. M. Höppener, C. J. M. Lips, and H. T. M. Timmers, “Menin links estrogen receptor activation to histone H3K4 trimethylation,” *Cancer Res.*, vol. 66, no. 9, pp. 4929–4935, 2006.

[12] N. Flynn, A. Getz, F. Visser, T. A. Janes, and N. I. Syed, “Menin: A tumor suppressor that mediates postsynaptic receptor expression and Synaptogenesis between central neurons of Lymnaea stagnalis,”

PLoS One, vol. 9, no. 10, pp. 11–16, 2014.

[13] F. Marini, “Genetic test in multiple endocrine neoplasia type 1 syndrome: An evolving story,” *World J. Exp. Med.*, vol. 5, no. 2, p. 124, 2015.

[14] G. Piecha, J. Chudek, and A. Więcek, “Primary hyperparathyroidism in patients with multiple endocrine neoplasia type 1.,” *Int. J. Endocrinol.*, vol. 2010, p. 928383, 2010.

[15] R. W. Schnepp *et al.*, “Mutation of tumor suppressor gene Men1 acutely enhances proliferation of pancreatic islet cells,” *Cancer Res.*, vol. 66, no. 11, pp. 5707–5715, 2006.

[16] Jessica Costa-Guda and Andrew Arnold, “Genetic and Epigenetic Changes in Sporadic Endocrine Tumors: Parathyroid Tumors Jessica,” *Mol Cell Endocrinol.*, vol. 386, no. 9, pp. 46–54, 2014.

[17] A. A. Hsi ED1, Zukerberg LR, Yang WI, “Cyclin D1/PRAD1 expression in parathyroid adenomas: an immunohistochemical study,” *J Clin Endocrinol Metab.*, vol. 81, no. 5, pp. 1736–9, 1996.

[18] Y. Imanishi *et al.*, “Primary hyperparathyroidism caused by parathyroid-targeted overexpression of cyclin D1 in transgenic mice,” *J. Clin. Invest.*, vol. 107, no. 9, pp. 1093–1102, 2001.

[19] R. a Chen and W. G. Goodman, “Role of the calcium-sensing receptor in parathyroid gland physiology.,” *Am. J. Physiol. Renal Physiol.*, vol. 286, no. 6, pp. F1005–F1011, 2004.

[20] O. Kifor *et al.*, “A syndrome of hypocalciuric hypercalcemia caused by autoantibodies directed at the calcium-sensing receptor,” *J. Clin. Endocrinol. Metab.*, vol. 88, no. 1, pp. 60–72, 2003.

[21] W. F. S. John M. Sharretts, Electron Kebebew, “Parathyroid Cancer,” *Semin Oncol.*, vol. 37, no. 6, pp. 580–590, 2010.

[22] K. Duan and O. Mete, “Parathyroid carcinoma: diagnosis and clinical implications,” *Turkish J. Pathol.*, vol. 3, pp. 80–97, 2015.

[23] Shaheera Shakeel and Muhammed Mubarak, “Proliferative Lesions of Parathyroid Glands: An Update for Practicing Pathologists.”

[24] C. Marcocci, F. Cetani, M. R. Rubin, S. J. Silverberg, A. Pinchera, and J. P. Bilezikian, “Parathyroid carcinoma,” *J. Bone Miner. Res.*, vol. 23, no. 12, pp. 1869–1880, 2008.

[25] F. Cetani *et al.*, “Genetic analyses of the HRPT2 gene in primary hyperparathyroidism: Germline and somatic mutations in familial and sporadic parathyroid tumors,” *J. Clin. Endocrinol. Metab.*, vol. 89, no. 11, pp. 5583–5591, 2004.

[26] F. Cetani *et al.*, “Should parafibromin staining replace HRTP2 gene analysis as an additional tool for histologic diagnosis of parathyroid carcinoma?,” *Eur. J. Endocrinol.*, vol. 156, no. 5, pp. 547–554, 2007.

[27] V. Guarnieri *et al.*, “Erratum: Large intragenic deletion of CDC73 (exons 4-10) in a three-generation hyperparathyroidism-jaw tumor (HPT-JT) syndrome family [BMC Med Genet. 2017;18:83] DOI

10.1186/s12881-017-0445-0," *BMC Med. Genet.*, vol. 18, no. 1, pp. 1–9, 2017.

[28] A. Takahashi *et al.*, "SHP2 Tyrosine Phosphatase Converts Parafibromin/Cdc73 from a Tumor Suppressor to an Oncogenic Driver," *Mol. Cell*, vol. 43, no. 1, pp. 45–56, 2011.

[29] L. Lin, J.-H. Zhang, L. M. Panicker, and W. F. Simonds, "The parafibromin tumor suppressor protein inhibits cell proliferation by repression of the c-myc proto-oncogene.," *Proc. Natl. Acad. Sci. U. S. A.*, vol. 105, no. 45, pp. 17420–5, 2008.

[30] W. T. Kassahun and S. Jonas, "Focus on parathyroid carcinoma," *Int. J. Surg.*, vol. 9, no. 1, pp. 13–19, 2011.

[31] J. Svedlund *et al.*, "Aberrant WNT/β-catenin signaling in parathyroid carcinoma," *Mol. Cancer*, vol. 9, no. 1, p. 294, 2010.

[32] J. Graff, D. Kim, M. M. Dobbin, and L. Tsai, "Epigenetic Regulation of Gene Expression in Physiological and Pathological Brain Processes," *Physiol. Rev.*, pp. 603–649, 2011.

[33] Weinhold B., "Epigenetics: the science of changes," *Env. Heal. Perspect*, vol. 114, no. 3, pp. 160–167, 2006.

[34] G. Egger, G. Liang, A. Aparicio, and P. A. Jones, "Epigenetics in human disease and prospects for epigenetic therapy," *Nature*, vol. 429, no. 6990, pp. 457–463, 2004.

[35] S. Sharma, T. K. Kelly, and P. A. Jones, "Epigenetics in cancer," *Carcinogenesis*, vol. 31, no. 1, pp. 27–36, 2009.

[36] R. Jaenisch and A. Bird, "Epigenetic regulation of gene expression: How the genome integrates intrinsic and environmental signals," *Nat. Genet.*, vol. 33, no. 3S, pp. 245–254, 2003.

[37] F. Watt and P. L. Molloy, "Cytosine methylation prevents binding to DNA of a HeLa cell transcription factor required for optimal expression of the adenovirus major late promoter.," *Genes Dev.*, vol. 2, no. 9, pp. 1136–1143, 1988.

[38] P. W. Laird, "The power and the promise of DNA methylation markers," *Nat. Rev. Cancer*, vol. 3, no. 4, pp. 253–266, 2003.

[39] T. Vaissiére and C. A. Miller, "DNA methylation: Dynamic and stable regulation of memory," *Biomol. Concepts*, vol. 2, no. 6, pp. 459–467, 2011.

[40] K. D. Robertson and A. P. Wolffe, "DNA methylation in health and disease," *Nat. Rev. Genet.*, vol. 1, p. 11, Oct. 2000.

[41] R. J. Klose and A. P. Bird, "Genomic DNA methylation: the mark and its mediators," *Trends Biochem. Sci.*, vol. 31, no. 2, pp. 89–97, 2006.

[42] N. Ahuja, Q. Li, A. L. Mohan, S. B. Baylin, and J.-P. J. Issa, "Aging and DNA methylation in colorectal mucose and cancer," *Cancer Res.*, vol. 58, no. 23, pp. 5489–5494, 1998.

[43] L. Z. Strichman-almashanu *et al.*, "A Genome-Wide Screen for Normally Methylated Human CpG Islands That Can Identify Novel

Imprinted Genes A Genome-Wide Screen for Normally Methylated Human CpG Islands That Can Identify Novel Imprinted Genes," no. March, pp. 543–554, 2002.

[44] N. A. Villota-Salazar, A. Mendoza-Mendoza, and J. M. González-Prieto, "Epigenetics: from the past to the present," *Front. Life Sci.*, vol. 9, no. 4, pp. 347–370, 2016.

[45] S. Golbabapour, N. A. Majid, P. Hassandarvish, M. Hajrezaie, M. A. Abdulla, and A. H. A. Hadi, "Gene Silencing and Polycomb Group Proteins: An Overview of their Structure, Mechanisms and Phylogenetics," *Omi. A J. Integr. Biol.*, vol. 17, no. 6, pp. 283–296, 2013.

[46] E. I. Campos and D. Reinberg, "New chaps in the histone chaperone arena," *Genes Dev.*, vol. 24, no. 13, pp. 1334–1338, 2010.

[47] V. Morales and H. Richard-Foy, "Role of Histone N-Terminal Tails and Their Acetylation in Nucleosome Dynamics.," *Mol. Cell. Biol.*, vol. 20, no. 19, pp. 7230–7237, 2000.

[48] A. J. Bannister, R. Schneider, and T. Kouzarides, "Histone methylation: Dynamic or static?," *Cell*, vol. 109, no. 7, pp. 801–806, 2002.

[49] S. Golbabapour, M. A. Abdulla, and M. Hajrezaei, *A concise review on epigenetic regulation: Insight into molecular mechanisms*, vol. 12, no. 12. 2011.

[50] P. Cheung and P. Lau, "Epigenetic Regulation by Histone Methylation and Histone Variants," *Mol. Endocrinol.*, vol. 19, no. 3, pp. 563–573, 2005.

[51] S. D. Taverna, H. Li, A. J. Ruthenburg, C. D. Allis, and D. J. Patel, "How chromatin-binding modules interpret histone modifications: lessons from professional pocket pickers," *Nat. Struct. &Amp; Mol. Biol.*, vol. 14, p. 1025, Nov. 2007.

[52] A. Sparmann and M. van Lohuizen, "Polycomb silencers control cell fate, development and cancer," *Nat. Rev. Cancer*, vol. 6, p. 846, Nov. 2006.

[53] A. M. Pietersen and M. van Lohuizen, "Stem cell regulation by polycomb repressors: postponing commitment," *Curr. Opin. Cell Biol.*, vol. 20, no. 2, pp. 201–207, 2008.

[54] J. A. Simon and C. A. Lange, "Roles of the EZH2 histone methyltransferase in cancer epigenetics," *Mutat. Res. Mol. Mech. Mutagen.*, vol. 647, no. 1, pp. 21–29, 2008.

[55] J. A. Simon and R. E. Kingston, "Mechanisms of Polycomb gene silencing: knowns and unknowns," *Nat. Rev. Mol. Cell Biol.*, vol. 10, p. 697, Sep. 2009.

[56] Z. Li, R. Cao, M. Wang, M. P. Myers, Y. Zhang, and R. M. Xu, "Structure of a Bmi-1-Ring1B polycomb group ubiquitin ligase complex," *J. Biol. Chem.*, vol. 281, no. 29, pp. 20643–20649, 2006.

[57] X. Nan *et al.*, “Transcriptional repression by the methyl-CpG-binding protein MeCP2 involves a histone deacetylase complex,” *Nature*, vol. 393, p. 386, May 1998.

[58] J. H. A. Vissers, M. van Lohuizen, and E. Citterio, “The emerging role of Polycomb repressors in the response to DNA damage,” *J. Cell Sci.*, vol. 125, no. 17, pp. 3939–3948, 2012.

[59] B. Xhemalce, M. A. Dawson, and A. J. Bannister, “Histone Modifications,” *Reviews in Cell Biology and Molecular Medicine*. 10-Oct-2011.

[60] P. A. Marks, V. M. Richon, T. Miller, and W. K. B. T.-A. in C. R. Kelly, “Histone Deacetylase Inhibitors,” vol. 91, Academic Press, 2004, pp. 137–168.

[61] S. Ropero and M. Esteller, “The role of histone deacetylases (HDACs) in human cancer,” *Mol. Oncol.*, vol. 1, no. 1, pp. 19–25, 2007.

[62] M. Oki, H. Aihara, and T. Ito, *Role Of Histone Phosphorylation In Chromatin Dynamics And Its Implications in Diseases*, vol. 41. 2007.

[63] F. F. Costa, “Non-coding RNAs: Lost in translation?,” *Gene*, vol. 386, no. 1, pp. 1–10, 2007.

[64] L. J. Collins, “The RNA infrastructure: An introduction to ncRNA networks,” *Adv. Exp. Med. Biol.*, vol. 722, pp. 1–19, 2011.

[65] J. W. Wei, K. Huang, C. Yang, and C. S. Kang, “Non-coding RNAs as regulators in epigenetics (Review),” *Oncol. Rep.*, vol. 37, no. 1, pp. 3–9, 2017.

[66] T. R. Mercer, M. E. Dinger, and J. S. Mattick, “Long non-coding RNAs: insights into functions,” *Nat. Rev. Genet.*, vol. 10, p. 155, Mar. 2009.

[67] P. Kapranov *et al.*, “RNA Maps Reveal New RNA Classes and a Possible Function for Pervasive Transcription,” *Science (80-.).*, vol. 316, no. 5830, p. 1484 LP-1488, Jun. 2007.

[68] F. P. Marchese, I. Raimondi, and M. Huarte, “The multidimensional mechanisms of long noncoding RNA function,” *Genome Biol.*, vol. 18, no. 1, pp. 1–13, 2017.

[69] C. P. Ponting, P. L. Oliver, and W. Reik, “Evolution and Functions of Long Noncoding RNAs,” *Cell*, vol. 136, no. 4, pp. 629–641, 2009.

[70] C. P. Ponting, P. L. Oliver, and W. Reik, “Evolution and Functions of Long Noncoding RNAs,” *Cell*, vol. 136, no. 4, pp. 629–641, 2009.

[71] V. Tripathi *et al.*, “The nuclear-retained noncoding RNA MALAT1 regulates alternative splicing by modulating SR splicing factor phosphorylation,” *Mol. Cell*, vol. 39, no. 6, pp. 925–938, 2010.

[72] J. L. Huang, L. Zheng, Y. W. Hu, and Q. Wang, “Characteristics of long non-coding RNA and its relation to hepatocellular carcinoma,” *Carcinogenesis*, vol. 35, no. 3, pp. 507–514, 2014.

[73] A. Fatica and I. Bozzoni, “Long non-coding RNAs: new players in cell differentiation and development,” *Nat. Rev. Genet.*, vol. 15, p. 7, Dec. 2013.

[74] P. Fortes and K. V Morris, “Long noncoding RNAs in viral infections,” *Virus Res.*, vol. 212, pp. 1–11, 2016.
[75] C. Kanduri, “Long noncoding RNAs: Lessons from genomic imprinting,” *Biochim. Biophys. Acta - Gene Regul. Mech.*, vol. 1859, no. 1, pp. 102–111, 2016.
[76] K. C. Wang and H. Y. Chang, “Molecular Mechanisms of Long Noncoding RNAs,” *Mol. Cell*, vol. 43, no. 6, pp. 904–914, 2011.
[77] J. H. Yoon *et al.*, “Scaffold function of long non-coding RNA HOTAIR in protein ubiquitination,” *Nat. Commun.*, vol. 4, pp. 1–14, 2013.
[78] Y. Fang and M. J. Fullwood, “Roles, Functions, and Mechanisms of Long Non-coding RNAs in Cancer,” *Genomics, Proteomics Bioinforma.*, vol. 14, no. 1, pp. 42–54, 2016.
[79] K. C. Wang and H. Y. Chang, “Molecular Mechanisms of Long Noncoding RNAs,” *Mol. Cell*, vol. 43, no. 6, pp. 904–914, 2011.
[80] F. Mohammad, T. Mondal, and C. Kanduri, “Epigenetics of imprinted long noncoding RNAs.,” *Epigenetics*, vol. 4, no. 5, pp. 277–286, 2009.
[81] J. H. Yoon *et al.*, “Scaffold function of long non-coding RNA HOTAIR in protein ubiquitination,” *Nat. Commun.*, vol. 4, pp. 1–14, 2013.
[82] M. Huarte *et al.*, “A large intergenic noncoding RNA induced by p53 mediates global gene repression in the p53 response,” *Cell*, vol. 142, no. 3, pp. 409–419, 2010.
[83] M. Kino, D. E. Hur, T. Ichijo, N. Nader, and G. P. Chrousos, “Noncoding RNA Gas5 Is a Growth Arrest and Starvation- Associated Repressor of the Glucocorticoid Receptor,” *Sci. Signal.*, vol. 3, no. 107, pp. 1–16, 2010.
[84] V. Tripathi *et al.*, “The nuclear-retained noncoding RNA MALAT1 regulates alternative splicing by modulating SR splicing factor phosphorylation,” *Mol. Cell*, vol. 39, no. 6, pp. 925–938, 2010.
[85] T. Nagano and P. Fraser, “No-nonsense functions for long noncoding RNAs,” *Cell*, vol. 145, no. 2, pp. 178–181, 2011.
[86] R. A. Gupta *et al.*, “Long non-coding RNA HOTAIR reprograms chromatin state to promote cancer metastasis,” *Nature*, vol. 464, p. 1071, Apr. 2010.
[87] M.-C. Tsai *et al.*, “Long Noncoding RNA as Modular Scaffold of Histone Modification Complexes,” *Science (80-.).*, vol. 329, no. 5992, p. 689 LP-693, Aug. 2010.
[88] and Y. X. Y Kotake, T Nakagawa, K Kitagawa, S Suzuki, N Liu, M Kitagawa, “NIH Public Access,” *Oncogene.*, vol. 30, no. 16, pp. 1956–1962, 2011.
[89] P. A. Jones and P. W. Laird, “Cancer-epigenetics comes of age,” *Nat. Genet.*, vol. 21, p. 163, Feb. 1999.
[90] P. A. Jones and S. B. Baylin, “The fundamental role of epigenetic events in cancer,” *Nat. Rev. Genet.*, vol. 3, p. 415, Jun. 2002.
[91] A. P. Feinberg, R. Ohlsson, and S. Henikoff, “The epigenetic

progenitor origin of human cancer," *Nat. Rev. Genet.*, vol. 7, p. 21, Jan. 2006.

[92] J. G. Herman, "Hypermethylation of tumor suppressor genes in cancer," *Semin. Cancer Biol.*, vol. 9, no. 5, pp. 359–367, 1999.

[93] Y. Schlesinger *et al.*, "Polycomb-mediated methylation on Lys27 of histone H3 pre-marks genes for de novo methylation in cancer," *Nat. Genet.*, vol. 39, p. 232, Dec. 2006.

[94] A. J. Bannister and T. Kouzarides, "Regulation of chromatin by histone modifications," *Cell Res.*, vol. 21, no. 3, pp. 381–395, 2011.

[95] M. Morlando and A. Fatica, "Alteration of epigenetic regulation by long noncoding RNAs in cancer," *Int. J. Mol. Sci.*, vol. 19, no. 2, 2018.

[96] A. M. Schmitt and H. Y. Chang, "Long Noncoding RNAs in Cancer Pathways," *Cancer Cell*, vol. 29, no. 4, pp. 452–463, 2016.

[97] M. Y. Shah and G. A. Calin, "The Mix of Two Worlds: Non-Coding RNAs and Hormones," *Nucleic Acid Ther.*, vol. 23, no. 1, pp. 2–8, 2013.

[98] J. Kentwell, J. S. Gundara, and S. B. Sidhu, "Noncoding RNAs in Endocrine Malignancy," *Oncologist*, vol. 19, no. 5, pp. 483–491, 2014.

[99] V. Guarnieri, L. A. Muscarella, C. Verdelli, and S. Corbetta, "Alterations of DNA methylation in parathyroid tumors," *Mol. Cell. Endocrinol.*, vol. 469, pp. 60–69, 2018.

[100] V. Chiara and C. Sabrina, "Epigenetics of human parathyroid tumors," *Int. J. Endocr. Oncol.*, vol. 4, no. 2, pp. 103–111, May 2017.

[101] L. F. Starker *et al.*, "The DNA methylome of benign and malignant parathyroid tumors," *Genes Chromosom. Cancer*, vol. 50, no. 9, pp. 735–745, 2011.

[102] J. Svedlund, S. K. Edblom, V. E. Marquez, G. Åkerström, P. Björklund, and G. Westin, "Hypermethylated in cancer 1 (HIC1), a tumor suppressor gene epigenetically deregulated in hyperparathyroid tumors by histone H3 lysine modification," *J. Clin. Endocrinol. Metab.*, vol. 97, no. 7, pp. 1307–1315, 2012.

[103] V. Vaira *et al.*, "The microRNA cluster C19MC is deregulated in parathyroid tumours," *J. Mol. Endocrinol.*, vol. 49, no. 2, pp. 115–124, 2012.

[104] S. Corbetta *et al.*, "Differential expression of microRNAs in human parathyroid carcinomas compared with normal parathyroid tissue," *Endocr. Relat. Cancer*, vol. 17, no. 1, pp. 135–146, 2010.

[105] C. Verdelli *et al.*, "The aberrantly expressed miR-372 partly impairs sensitivity to apoptosis in parathyroid tumor cells.," *Endocr. Relat. Cancer*, May 2018.

[106] V. Guarnieri *et al.*, "CDC73 mutations and parafibromin immunohistochemistry in parathyroid tumors: Clinical correlations in a single-centre patient cohort," *Cell. Oncol.*, vol. 35, no. 6, pp. 411–422, 2012.

[107] F. Cetani *et al.*, “CDC73 mutational status and loss of parafibromin in the outcome of parathyroid cancer,” *Endocr. Connect.*, vol. 2, no. 4, pp. 186–195, 2013.
[108] F. B. Rodrigues *et al.*, “Her Aching Bones: Atypical Parathyroid Adenoma,” *Am. J. Med.*, vol. 129, no. 3, pp. 260–262, 2016.
[109] T. Dwight *et al.*, “Loss of heterozygosity in sporadic parathyroid tumours: involvement of chromosome 1 and the MEN1 gene locus in 11q13.,” *Clin. Endocrinol. (Oxf).*, vol. 53, no. 1, pp. 85–92, Apr. 2002.
[110] E. Friedman *et al.*, “Allelic Loss from Chromosome 11 in Parathyroid Tumors,” vol. 52, pp. 6804–6809, 1992.
[111] Y. Kondo, “Targeting histone methyltransferase EZH2 as cancer treatment,” *J. Biochem.*, vol. 156, no. 5, pp. 249–257, 2014.
[112] L. E. Moritz and R. C. Trievel, “Structure, mechanism, and regulation of polycomb repressive complex 2,” *J. Biol. Chem.*, p. jbc.R117.800367, 2017.
[113] K. S. Pollard *et al.*, “An RNA gene expressed during cortical development evolved rapidly in humans,” *Nature*, vol. 443, p. 167, Aug. 2006.
[114] R. Johnson *et al.*, “Human accelerated region 1 noncoding RNA is repressed by REST in Huntington’s disease,” *Physiol. Genomics*, vol. 41, no. 3, pp. 269–274, 2010.
[115] M. I. Alvelos *et al.*, “MEN1 intragenic deletions may represent the most prevalent somatic event in sporadic primary hyperparathyroidism,” *Eur. J. Endocrinol.*, vol. 168, no. 2, pp. 119–128, 2013.
[116] B. Xu *et al.*, “Tumor suppressor menin represses Paired box gene 2 expression via Wilms tumor suppressor protein-Polycomb group complex,” *J. Biol. Chem.*, vol. 286, no. 16, pp. 13937–13944, 2011.
[117] L. Huss, S. Butt, S. Borgquist, M. Almquist, J. Malm, and J. Manjer, “Serum levels of vitamin D, parathyroid hormone and calcium in relation to survival following breast cancer,” *Cancer Causes Control*, vol. 25, no. 9, pp. 1131–1140, 2014.
[118] M. D. Spandana J. Brown, M.D.; Mary D. Ruppe, M.D.; Laila S. Tabatabai, “THE PARATHYROID GLAND AND HEART DISEASE,” *MDCVJ*, vol. XIII (2), 2017.
[119] H. K. Mohan, A. M. Groves, I. Fogelman, and S. E. M. Clarke, “Thyroid Hormone and Parathyroid Hormone Competing to Maintain Calcium Levels in the Presence of Vitamin D Deficiency,” *Thyroid*, vol. 14, no. 9, pp. 789–791, Sep. 2004.
[120] C. H Wei and A. Harari, *Parathyroid Carcinoma: Update and Guidelines for Management*, vol. 13. 2012.
[121] V. García-Carpizo, L. Ruiz-Llorente, M. Fraga, and A. Aranda, “The growing role of gene methylation on endocrine function,” *J. Mol. Endocrinol.*, vol. 47, no. 2, 2011.
[122] S. Rodríguez-Rodero, E. Delgado-Álvarez, A. F. Fernández, J. L.

Fernández-Morera, E. Menéndez-Torre, and M. F. Fraga, “Epigenetic alterations in endocrine-related cancer,” *Endocr. Relat. Cancer*, vol. 21, no. 4, 2014.

[123] P. J. Batista and H. Y. Chang, “Long noncoding RNAs: Cellular address codes in development and disease,” *Cell*, vol. 152, no. 6, pp. 1298–1307, 2013.

[124] T. Derrien *et al.*, “The GENCODE v7 catalog of human long noncoding RNAs : Analysis of their gene structure , evolution , and expression,” pp. 1775–1789, 2012.

[125] E. P. Booy, E. K. S. McRae, A. Koul, F. Lin, and S. A. McKenna, “The long non-coding RNA BC200 (BCYRN1) is critical for cancer cell survival and proliferation,” *Mol. Cancer*, vol. 16, no. 1, pp. 1–15, 2017.

[126] W. F. Simonds, “Parathyroid cancer and the CDC73 tumor suppressor gene,” *Int. J. Endocr. Oncol.*, vol. 1, no. 1, pp. 59–69, Aug. 2014.

[127] I. Kikuchi *et al.*, “Dephosphorylated parafibromin is a transcriptional coactivator of the Wnt/Hedgehog/Notch pathways,” *Nat. Commun.*, vol. 7, pp. 1–15, 2016.

[128] A. Ramaswamy, T. Vijitha, B. Kumarguru, and P. Mahalingashetti, “Atypical parathyroid adenoma,” *Indian J. Pathol. Microbiol.*, vol. 60, no. 1, pp. 99–101, Jan. 2017.

[129] Y. Shi, J. Hogue, D. Dixit, J. Koh, and J. A. Olson, “Functional and genetic studies of isolated cells from parathyroid tumors reveal the complex pathogenesis of parathyroid neoplasia,” *Proc. Natl. Acad. Sci.*, vol. 111, no. 8, pp. 3092–3097, 2014.

[130] L. Forsberg *et al.*, “Distinction in gene expression profiles demonstrated in parathyroid adenomas by high-density oligoarray technology,” *Eur. J. Endocrinol.*, vol. 152, no. 3, pp. 459–470, 2005.

[131] B.-Y. Kim *et al.*, “Genetic analysis of parathyroid and pancreatic tumors in a patient with multiple endocrine neoplasia type 1 using whole-exome sequencing,” *BMC Med. Genet.*, vol. 18, no. 1, p. 106, 2017.

[132] C. H. Waddington, “An introduction to modern genetics,” *Eugen. Rev.*, vol. 31, no. 4, p. 218, 1940.

[133] R. Margueron *et al.*, “Role of the polycomb protein EED in the propagation of repressive histone marks,” *Nature*, vol. 461, p. 762, Sep. 2009.

[134] S. Kaneko *et al.*, “Phosphorylation of the PRC2 component Ezh2 is cell cycle-regulated and up-regulates its binding to ncRNA,” *Genes Dev.*, vol. 24, no. 23, pp. 2615–2620, 2010.

[135] A. Schumacher, O. Lichtarge, S. Schwartz, and T. Magnuson, “The MurinePolycomb-Group Geneeedand Its Human Orthologue: Functional Implications of Evolutionary Conservation,” *Genomics*, vol. 54, no. 1, pp. 79–88, 1998.

[136] S. C. Hsu, J. Galceran, and R. Grosschedl, “Modulation of

transcriptional regulation by LEF-1 in response to Wnt-1 signaling and association with beta-catenin.," *Mol. Cell. Biol.*, vol. 18, no. 8, pp. 4807–18, 1998.

[137] C. Jamieson, C. Lui, M. G. Brocardo, E. Martino-Echarri, and B. R. Henderson, "Rac1 augments Wnt signaling by stimulating -catenin-lymphoid enhancer factor-1 complex assembly independent of -catenin nuclear import," *J. Cell Sci.*, vol. 128, no. 21, pp. 3933–3946, 2015.

8. SITOGRAPHY

1. https://www.genecards.org/
2. https://www.parathyroid.com/
3. https://clinicaltrials.gov (NIH_U.S. National Library of Medicine)
4. https://rarediseases.info.nih.gov/
5. https://string-db.org/
6. http://projects.tcag.ca/variation/

9. SCIENTIFIC PRODUCTS

Verdelli C, Forno I, Morotti A, Creo P, Guarnieri V, Scillitani A, Cetani F, Vicentini L, Balza G, Beretta E, Ferrero S, Vaira V, Corbetta S. The aberrantly expressed miR-372 partly impairs sensitivity to apoptosis in parathyroid tumor cells (2018). ***Endocrine-Related Cancer*** 25(7):761-771. doi: 10.1530/ERC-17-0204.

Del Gobbo A, Morotti A, Colombo AE, Vaira V, Ercoli G, Pesenti C, Bonaparte E, Guerini-Rocco E, Di Cristofori A, Locatelli M, Palleschi A, Ferrero S. IMP3 expression in NSCLC brain metastasis demonstrates its role as a prognostic factor in non-neuroendocrine phenotypes (2017). ***Medical Oncology*** 35(1):2 doi: 10.1007/s12032-017-1062-7.

Caino MC, Seo JH, Aguinaldo A, Wait E, Bryant KG, Kossenkov AV, Hayden JE, Vaira V, Morotti A, Ferrero S, Bosari S, Gabrilovich DI, Languino LR, Cohen AR, Altieri DC. A neuronal network of mitochondrial dynamics regulates metastasis (2016). ***Nature Communications*** 7:3730 doi: 10.1038.

Presentations

Poster presentation at 25th biennial congress of EACR (Amsterdam, 2018). 'Interplay between coding and non-coding genome in parathyroid tumors'.

Poster presentation at AACR Annual Meeting (Chicago, 2018). 'Insights into the non-coding genome in human parathyroid tumors'.

Poster presentation at the Biennial Congress of the Italian Association of Cell Biology and Differentiation (Bologna, 2017). 'Long non-coding RNAs expression profiling in human parathyroid tumors'.

Poster presentation at EACR-AACR-SIC special conference (Florence, 2017). 'Long non-coding RNAs: a new class of diagnostic biomarkers in human parathyroid tumors'.

Work selected for an oral presentation at 20th European Congress of Endocrinology (Barcelona, 2018). 'LncRNAs profiling reveals epigenetic heterogeneity among human parathyroid tumors'.

Work selected for poster presentation at 19th European Congress of Endocrinology (Lisbon, 2017). 'Long non-coding RNA expression profiles in human parathyroid tumors'.

Awards

June 2017 - **Travel grant at EACR-AACR-SIC congress** - The challenges of optimizing immune and targeted therapies: from cancer biology to the clinic (Florence, 2017).

May 2017 - **Poster prize at 19th European Congress of Endocrinology** (Lisbon, 2017).